

**GRAPHENE TRANSFER APPROACHES
WITH DIFFERENT SUPPORT MATERIALS
ON THE SUBSTRATES WITH CAVITIES**

**A Thesis Submitted to
the Graduate School of Engineering and Sciences of
İzmir Institute of Technology
in Partial Fulfillment of the Requirements for the Degree of**

MASTER OF SCIENCE

in Electronics and Communication Engineering

**by
Sinem Duman**

**July 2019
İZMİR**

We approve the thesis of **Sinem DUMAN**

Examining Committee Members:



Assoc. Prof. Dr. Müjdat BALANTEKİN

Department of Electrical and Electronics Engineering, İzmir Institute of Technology



Assoc. Prof. Dr. Alev Devrim GÜÇLÜ

Department of Physics, İzmir Institute of Technology



Asst. Prof. Dr. Gökhan UTLU

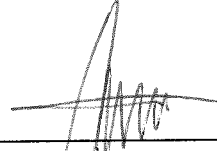
Department of Physics, Ege University

18 July 2019



Assoc. Prof. Dr. Müjdat BALANTEKİN

Supervisor, Department of Electrical and Electronics Engineering, İzmir Institute of Technology



Assoc. Prof. Dr. Cem ÇELEBİ

Co-Supervisor, Department of Physics, İzmir Institute of Technology



Prof. Dr. Enver TATLICIOĞLU

Head of the Department of Electrical and Electronics Engineering

Prof. Dr. Aysun SOFUOĞLU

Dean of the Graduate School of Engineering and Sciences

ACKNOWLEDGMENTS

I had a great chance to do research with three research groups and four mentors. First of all, I would like to thank and honor memorable mentor, Assoc. Prof. Dr. Yusuf Selamet. Because of his lovely support and great guidance.

I would like to express my appreciate to my supervisor Assoc. Prof. Dr. Müjdat Balantekin. I really appreciate his guidance and interest in this study. He introduced the MEMS area to me and I also learned a lot from him.

My co-advisor Assoc. Prof. Dr Cem Çelebi, I would like to thank him for giving me the opportunity of doing this study in the Quantum Device Laboratory (QDL) and for his valuable support, trust and guidance during the study. I greatly profited from his experimental intuition and solid background about semiconductor device physics.

I was also so lucky enough to experience a research at Wide Bandgap Semiconductors (SC2G) research group about diamond MOSCAP structures. I am very grateful for this unique experience and would like to sincerely thank to Etienne Gheeraert, David Eon and Julien Pernot for their valuable guidance during my sixth months of MSc. training.

Furthermore, I would like to thank the committee members of this thesis: Assoc. Prof. Dr. A. Devrim Güçlü and Asst. Prof. Dr. Gökhan Utlü for their contribution of constructive comments on the manuscript.

I would like to thank TÜBİTAK for funding this research under project no. 117F186, İzmir Institute of Technology, Center for Materials Research for AFM and SEM analyses and trainings, and Middle East Technical University Micro-Electro-Mechanical Systems Research and Application Center (METU-MEMS) for fabrication of cavity structures. Moreover, I would like to warmly acknowledge the IZTECH BioSens & BioApps research group for providing PDMS material.

I would like to thank all the lab friends from QDL research group. I also would like to express my deep gratitude to Mine Bahçeci for AFM analyses. I also would like to warmly acknowledge Firat Bakır for his support with CAD tools and teaching me AutoCad.

Finally, none of the words I could possibly find would sufficiently describe how much I owe to my family. I am extremely lucky to have such loving parents. I deeply and sincerely thank them for standing by my side and for their unconditional support and encouragement.

ABSTRACT

GRAPHENE TRANSFER APPROACHES WITH DIFFERENT SUPPORT MATERIALS ON THE SUBSTRATES WITH CAVITIES

A micro capacitive sensor characteristically embraces a thin conductive membrane which is freely suspended above an immovable counter electrode in a parallel plate geometry. Such capacitive structures are found in broad range of applications as a transducer like capacitive micro-machined ultrasonic transducer (CMUT), pressure sensor, resonator and biological or chemical material sensing element. The input can be an ultrasound wave, pressure, chemical or biological mass attachment which result in the deflection of the membrane.

Emerging nano materials have shown great potential as candidates for generation of nano and micro electromechanical systems (NEMS, MEMS). Among these nano materials, graphene is regarded as a promising material because of its ultra low mass, thickness, high surface to volume ratio, flexibility, and extraordinary electrical and mechanical properties. However, the transfer of graphene on substrates with micro scale cavities is challenging since the fabrication of large area membranes with a smaller air gap often results in membrane tearing or collapse driven by capillary or electrostatic forces.

This study presents a research on the fabrication and the characterization of graphene membranes to be used in micro capacitive sensor applications. Substrates which span a large array of circular and hexagonal micro cavities between 2-100 μm in diameter are fabricated. Graphene transfer with different support materials are studied to fabricate graphene micro membranes. Up to 5 μm diameter membranes on 300 nm deep cavities are demonstrated via scanning electron microscope (SEM) and atomic force microscope (AFM) tools.

ÖZET

OYUKLU ALT TAŞLAR ÜZERİNDE FARKLI DESTEK MALZEMELERİ İLE GRAFEN AKTARMA YAKLAŞIMLARI

Mikro kapasitif sensör, karakteristik olarak, iletken ve hareketsiz duran bir alt elektrot ile buna paralel olarak yerleştirilmiş iletken ve hareket edebilen bir üst elektrottan oluşur. Bu yapı, kapasitif mikro- işlenmiş ultrasonik çevirgeç, basınç sensörü, resonatör ve biyolojik yada kimyasal madde algılama elemanı gibi uygulamalarda dönüştürücü olarak bulunabilir. Membran yapısında eğilmeye yol açan fiziksel girdi ultrason dalgası, basınç, biyolojik yada kimyasal bir malzeme olabilir.

Nano malzemeler, yeni nesil nano ve mikro elektro mekanik sistemlerin (NEMS, MEMS) geliştirilmesinde büyük potansiyele sahiptir. Nano malzemelerin arasında grafen çok küçük kütlesi, yüksek yüzey hacim oranı, esnekliği, özel elektriksel ve mekanik özelliklerinden dolayı öne çıkan bir malzemedir. Ancak, grafenin kapasitif yapılar oluşturmak üzere mikro ölçekte oyuklu örnekler üzerine aktarılması kılcal veya elektrosatik kuvvetlerin etkisinden ötürü membran yapısının çökmesi veya yırtılması ile sonuçlanabilir.

Bu çalışma, kapasitif mikro sensor olarak kullanılmak üzere çok ince grafen membranlarının oluşturulmasını ve karakterizasyonunu içermektedir. Bu amaç ile çapları 2 ile 100 μm arasında değişen değişikli alttaşlar hazırlanmıştır. Grafen mikro membran üretimi için, farklı destek malzemeleri kullanılarak, grafen transferi gerçekleştirilmiştir. 300 nm derinliğinde değişikli yapılar üzerinde çapları 5 μm 'ye kadar ulaşan grafen membranlar taramalı elektron ve atomik kuvvet mikroskobu ölçümleri ile gösterilmiştir.

TABLE OF CONTENTS

LIST OF FIGURES	viii
LIST OF TABLES	xi
LIST OF ABBREVIATIONS	xii
CHAPTER 1. INTRODUCTION	1
CHAPTER 2. GRAPHENE MEMBRANES AND THEIR APPLICATIONS	3
2.1. Graphene Membranes	3
2.2. Applications of Graphene Membranes	3
CHAPTER 3. GRAPHENE AND SUSPENDED GRAPHENE: PROPERTIES, SYNTHESIS AND TRANSFER	6
3.1. Graphene: A 2D Material	6
3.2. Crystal and Band Structure of Graphene	6
3.3. Important Properties of Graphene	7
3.4. Mechanical Properties of Graphene and Suspended Graphene	7
3.5. Synthesis of Graphene	8
3.5.1. Mechanical Exfoliation Method	9
3.5.2. Chemical Vapour Deposition Method	10
3.6. Transfer of CVD Synthesized Graphene on Target Substrates	11
3.6.1. Transfer Approach 1: According to the Interaction Between Graphene and Target Substrate	12
3.6.2. Transfer Approach 2: According to the Additional Support Layer	13
CHAPTER 4. CHARACTERIZATION TECHNIQUES	19
4.1. Optical Microscopy	19
4.2. Scanning Electron Microscopy	19
4.3. Raman Spectroscopy	20
4.4. Atomic Force Microscopy	23

CHAPTER 5. TRANSFER APPROACHES TO FABRICATE GRAPHENE	
MICRO MEMBRANES	24
5.1. APCVD Synthesis of Graphene	24
5.1.1. Transfer of APCVD Grown Graphene on Flat Substrates.....	27
5.2. Fabrication of Substrates with Cavities	31
5.3. Support Materials for the transfer of APCVD Grown Graphene on the Substrates with Cavities	34
5.3.1. Photoresist	35
5.3.2. PMMA	36
5.3.3. Photoresist & PMMA	37
5.3.4. PDMS	38
5.3.5. PDMS & PMMA	39
5.3.6. Thermal Release Tape.....	40
5.3.7. Thermal Release Tape & PMMA.....	46
5.3.8. Discussion	46
 CHAPTER 6. CONCLUSION AND FUTURE WORK	 49
 REFERENCES	 51

LIST OF FIGURES

<u>Figure</u>	<u>Page</u>
Figure 3.1. Schematic of CVD growth of graphene (source: Kumar and Huei, 2013).	11
Figure 3.2. Schematic of graphene synthesis on Cu foil (source: Kumar and Huei, 2013).	12
Figure 3.3. Illustration of graphene synthesis on defects side of the foil, (a) dissolving of carbon atoms inside the defect sides at high temperatures, (b) the dissolved carbon atoms forms graphene layers during cooling down process, (c) SEM image showing the graphene layer number differences around the defect sides, (source: Graph, 2013).	13
Figure 3.4. Schematic of wet and dry transfer procedures (a) dry transfer onto cavities, wet transfer onto (b) perforated and (c) flat substrates. Dashed lines are for magnified images (source: Suk <i>et al.</i> , 2011).	14
Figure 3.5. Schematic of standard (left) and direct (right) transfer methods (source: Regan <i>et al.</i> , 2010).	15
Figure 3.6. Transfer of graphene on SiO ₂ substrates with cavities (10 and 110 μm in diameter) with PMMA support layer (source: Hwangbo <i>et al.</i> , 2014).	16
Figure 3.7. Transfer of graphene on SiO ₂ substrates with cavities with PMMA support layer (source: Lee <i>et al.</i> , 2014).	17
Figure 3.8. Methods for PMMA removal for fabricating free standing CVD graphene, (a) conventional (b) inverted floating method (source: Lee <i>et al.</i> , 2014). ..	18
Figure 3.9. Schematic presenting the fabrication of free standing CVD graphene with PMMA material (source: Berger <i>et al.</i> , 2017).	18
Figure 4.1. Optical microscope images of graphene layers on SiO ₂ /Si. Different thicknesses and light wavelengths results in different optical contrast and the contrast corresponds to layer number differences. Image sizes are 25 \times 25 μm (source: Blake <i>et al.</i> , 2007).	20
Figure 4.2. SEM images of circular drumhead graphene from top view (a) and 45° tilted (b) views. (c) and (d) show graphene over triangular trenches with 52° tilted view. All the graphene layers are on 290 nm SiO ₂ on Si substrate. All scale bars are 1 μm (source: Lee <i>et al.</i> , 2015).	21
Figure 4.3. Raman spectra for mono, bi, few layer graphene and graphite (HOPG) (source: Cantarero, 2015).	22

Figure 4.4. (a) SEM image of membranes over cavities changing between 1 and 1.5 μm in diameter with scale bar of 3 μm . I is partially covered, II is fully covered and III is fractured graphene. (b) noncontact AFM image of suspended graphene. Solid line is the height profile (2.5 nm) along the dashed line. (c) schematic showing the AFM nanoindentation technique. (d) noncontact AFM image of a fractured graphene membrane (source: Lee <i>et al.</i> , 2008).	23
Figure 5.1. APCVD growth unit (a) Lindberg Blue oven from Thermo Scientific Instruments (b) gas flow controller unit (c) Cu foils inside the growth chamber.	25
Figure 5.2. Temperature-Time graph presenting the mono-layer graphene growth steps with APCVD technique on Cu foil.	26
Figure 5.3. Optical microscope images of graphene after transferred on flat SiO ₂ samples (a) transferred via dry transfer approach with photoresist as support material, (b) transferred via wet transfer (fishing) approach with PMMA as a support material.	28
Figure 5.4. Mono and bi-layer graphene Raman spectrum.	29
Figure 5.5. Raman spectrum for the few and multi-layer graphene.	30
Figure 5.6. Schematic representation of micro cavity fabrication (a) cleaning of substrate on which the cavity structures will be fabricated, (b) spin coating of photoresist material, (c) UV lithography, (d) development of photoresist, (e) anisotropic etching of SiO ₂ layer with RIE technique, (f) Cr/Au deposition, (g) chemical removal of photoresist.	31
Figure 5.7. AFM height profile (approximately 300 nm) for a cavity with 35 μm diameter (left). Stylus profiler height profile (approximately 2 μm) for a cavity with 70 μm diameter (right).	32
Figure 5.8. Optical microscope images of cavity structures used in the thesis study. (a) 10 μm cavities, (b) 100 μm cavities, (c) circular cavities, (d) hexagonal cavities, (e) $R/10$ cavity distance with diameter R , (f) R cavity distance, (g) air gap device cavities, (h) vacuum gap device cavities, (i) and (j) show the cavities with different diameters.	33
Figure 5.9. Schematized standard transfer technique: (a) graphene on Cu foil, (b) coating a support material on graphene top layer, (c) chemical etching of Cu foil, (d) SiO ₂ /Si substrate with cavities where the graphene will be transferred on, (e) adhesion of the graphene on the target substrate	

(f) removal of the support material.	34
Figure 5.10. Schematic which illustrates detachments of carrier films during standard transfer method.	35
Figure 5.11. SEM image after graphene transfer on 10 μm cavity structure by using S1813 type photoresist material.	36
Figure 5.12. Optical microscope image of graphene transfer via PMMA support material on cavity structures of changing diameters.	37
Figure 5.13. 3D AFM height profile for a substrate before (a) and after (b) transfer. .	38
Figure 5.14. SEM image of mono-layer graphene transfer by using PDMS & PMMA heterostructure as a support material. (a) cavity structure with graphene layer after the transfer, (b) close up view of the same cavity indicated by red dashed square.	38
Figure 5.15. SEM image of structures with cavities after the transfer via thermal release tape.	39
Figure 5.16. SEM image of suspended (a) and broken (b) membrane structures, transferred via PDMS& PMMA support layer.	41
Figure 5.17. SEM image of (a) a ruptured and (b) broken mono-layer graphene membrane structures transferred via PDMS & PMMA support layer. ...	42
Figure 5.18. SEM image of a mono-layer graphene half membrane structure transferred with PDMS & PMMA support layer.	43
Figure 5.19. AFM height profile (top) and 3D image (bottom) of a graphene membrane over a 300 nm deep cavity with $\sim 2 \mu m$ diameter. White line on the right image shows the path where the height profile is taken.	43
Figure 5.20. AFM height profiles (first and second) and 3D images (third and forth) of $\sim 4 \mu m$ cavity structures before (left) and after (right) graphene transfer via PDMS & PMMA support layer.	44
Figure 5.21. AFM height profile and image of a graphene membrane over a 300 nm deep cavity with $\sim 5 \mu m$ diameter. White line on the right image shows the path where the height profile is taken.	45
Figure 5.22. Optical image of a mono-layer graphene transferred on cavity structures via thermal release tape as support material.	45
Figure 5.23. Optical microscope image of graphene transfer via thermal release tape & PMMA as support layer. Transfer is applied on samples which have cavity structures of changing diameters.	46

LIST OF TABLES

<u>Table</u>		<u>Page</u>
Table 3.1.	Important properties of graphene	8
Table 5.1.	Parameters used for APCVD graphene synthesis	26
Table 5.2.	Summary of transfer approaches used in this study	48

LIST OF ABBREVIATIONS

AFM	Atomic Force Microscopy
CMUT	Capacitive Micro-machined Ultrasonic Transducer
CVD	Chemical Vapor Deposition
DI	Deionized
SEM	Scanning Electron Microscope
MEMS	Micro Electromechanical Systems
NEMS	Nano Electromechanical Systems
PDMS	Polydimethylsiloxane
PMMA	Poly Methyl Methacrylate
RIE	Reactive Ion Etching
SEM	Scanning Electron Microscope
UV	Ultra Violet
2D	Two Dimensional
3D	Three Dimensional

CHAPTER 1

INTRODUCTION

There has been increasing scientific and technological interest in the miniaturization of mechanical systems, both in micro and nano meter scales, driven by the micro-electromechanical systems (MEMS) and nano-electromechanical systems (NEMS) fields. MEMS and NEMS investigate the behaviour and performance of integrated devices in the micrometer regime. Such devices are fabricated with specifically developed technologies with the aim of integrating electrical and mechanical components into one device to perform certain functions.

Dimensions of MEMS devices are in the range of few to hundreds of microns. MEMS devices can sense, control and actuate on the micro scale while generating an effect at the macro scale. Moreover, the dimensions and mass reduction in MEMS, naturally leads to higher sensitivity to external forces acting on them, making these systems very interesting for sensing applications (Cooper *et al.*, 2011). Suspended membranes over micro cavities are widely used as MEMS transducers (sensors and actuators). This kind of structures consist of a suspended plate or pendulum proof mass assembly and the sensing mechanism can be piezoresistive, piezoelectric, resonating or capacitive. These type of MEMS devices can be pressure sensors (Smith *et al.*, 2014), transducers like CMUTs (Chong *et al.*, 2014), resonators (Bunch *et al.*, 2007) and biomedical sensors (Zhu *et al.*, 2014) where the input signal can be a pressure difference, acoustic waves, biological or chemical particles or any other physical source which results with a pressure difference or deformation on the sensing element.

While the field of nano and micro technology has been quickly growing over the last few decades, the study of atomically thin (2D) materials increases the possibilities and functionality of MEMS and NEMS applications and devices. Graphene is the first and one of the most promising 2D material with one atom thickness and has remarkable applications due to the combination of its extraordinary strength, electric and thermal conductivity, optical transparency, flexibility and ultra low mass. Additionally, this exceptional material exhibits an extremely high surface to volume ratio. High strength, ultra-low mass, high surface to volume ratio and the flexibility of graphene make this 2D material an ideal candidate to push the limits for MEMS sensor technology. Understanding the mechanical properties of the suspended graphene membranes is very critical

for the development of graphene MEMS devices. Stiffness is an important parameter for noise and sensitivity of a capacitive sensor and depends on geometry and membrane material. High sensitivity could also be achieved with increasing diameters (membrane area). However, the transfer of graphene on micro cavities is a challenging procedure. Because, the fabrication of large area suspended graphene membrane structures with a smaller gap often results in membrane collapse driven by capillary or electrostatic forces.

This thesis reports a research about fabrication of micro membrane structures with graphene material as a top electrode to fabricate capacitive micro membranes. To fabricate a large array of circular and hexagonal micro cavities between 2 and 100 μm in diameter SiO_2/Si samples is patterned via optical lithography and etching was done with reactive ion etching (RIE) technique. As a back-plate electrode Si is used and the oxide layer on silicon used as support well for suspended graphene layer. Because of high uniformity, large area process ability and transferability, chemical vapour deposition (CVD) method is chosen for graphene synthesis. Different graphene transfer methods in terms of different graphene support materials are studied to fabricate such membrane structures.

The goals of the thesis can be stated as follows: Understanding the concepts related with graphene micro-membranes. Fabricating cavity structures of 2-100 μm in diameter and 300-2000 nm in depth. Fabricating suspended graphene structures in micro meter scale with different support layers during graphene transfer and characterization of fabricated structures.

This thesis is composed of the following sections: Chapter 2 provides a literature review on graphene micro membranes and their applications. Chapter 3 introduces graphene, describes its structure and important properties. Moreover, commonly used graphene synthesis methods are summarized and transfer methods used for fabricating suspended membranes are discussed. Chapter 4 introduces the characterization techniques for suspended graphene membrane structures. Chapter 5 presents the fabrication and characterization of graphene micro membranes. Chapter 6 summarizes the study and presents the planned future study.

CHAPTER 2

GRAPHENE MEMBRANES AND THEIR APPLICATIONS

2.1. Graphene Membranes

Membrane theory and applications with membranes are not a new topic but the current technology is based on thin films or silicon background. Graphene and other 2D materials are currently facilitating the development of ultra thin membrane sensor technologies opening a new field in NEMS and MEMS.

Meyer *et al.* (2007) demonstrated that individual graphene sheets with one atom thickness can be freely suspended on a micro fabricated scaffolds in vacuum or air. That was the first experimental observation showing that graphene crystals with long range crystalline order can exist without a substrate and exhibit elastic deformations in all three dimensions. After the first graphene membrane fabrication, a lot of experimental and theoretical work have been done to observe physical properties of graphene and fabricating suspended graphene membrane based devices. Membranes with mono-layer graphene have been fabricated in nano and micro scale (Arjmandi-Tash *et al.*, 2017; Meyer *et al.*, 2007). Furthermore, membrane with multilayer graphene layer was fabricated in milli meters scale (Lee *et al.*, 2014).

Understanding the mechanical properties of suspended graphene membranes is key to the development of graphene MEMS and NEMS devices. Because, as a 2D nano-material, graphene loses its unique (intrinsic) properties (especially mechanical) when it makes contact with bulk substrates (Bolotin *et al.*, 2008). Suspending graphene membranes over shallow wells or perforated substrates decrease substrate interactions and allows fundamental studies to find intrinsic properties of graphene like mechanical (Lee *et al.*, 2008; Frank *et al.*, 2007), electronic (Bolotin *et al.*, 2008) and structural (Bunch *et al.*, 2008) and more.

2.2. Applications of Graphene Membranes

In sensor applications, especially in NEMS and MEMS, the ones which are using the principle of electromechanical coupling, graphene as one of the 2D material, is advantageous because of its exceptional electronic and mechanical properties. For a membrane structure to be used in NEMS and MEMS, it is advantageous if the material is both strong and flexible. Moreover, the membrane thickness is correlated with sensitivity of membrane based devices. As the membrane thickness decreases, the sensitivity increases (Gong and Lee, 2001). That is why the excellent properties and one atom thickness make graphene an ideal candidate for such an applications summarized below.

Graphene membrane structures can be used in various kinds of applications such as separation barrier between two environments (Bunch *et al.*, 2008), pressure sensor (Sorkin and Zhang, 2011; Smith *et al.*, 2013) mechanical resonator (Bunch *et al.*, 2007; Van Der Zande *et al.*, 2010; Song *et al.*, 2012). For this kind of applications sensing mechanism can be piezoresistive, piezoelectric or resonating. The first graphene resonator was fabricated with exfoliated graphene over nm scale predefined trenches on silica substrate by Bunch *et al.* (2007). Besides, in the study reported by Smith *et al.* (2014), graphene membranes were fabricated over $6 \mu\text{m}$ by $64 \mu\text{m}$ cavities to fabricate pressure sensor using the piezoresistive effect in graphene.

Moreover, graphene can be found in applications based on capacitive sensing mechanism. Suspended graphene membrane structure can be used as capacitive micromachined ultrasonic transducer (CMUT) (Liu *et al.*, 2004), variable capacitor (AbdelGhany *et al.*, 2016) and gas, chemical or biological sample detector (Zhu *et al.*, 2014). The graphene can be hybridized and biocompatible, which opens the field of biosensing applications (Zhu *et al.*, 2014).

Capacitive micro-machined ultrasonic transducer (CMUT) transduces energy due to change in capacitance (Khuri-Yakub and Oralkan, 2011). The metallic thin layer suspended on the cavity structure acts as a top electrode together with metallic bottom layer acting as a bottom electrode. CMUT structure can found in applications like medical ultrasonic imaging, underwater imaging, flow measurement of liquids and gases or non-destructive testing. The membranes of CMUT's were generally fabricated with very thin silicon, silicon nitride or a metal (Liu *et al.*, 2004) until the rise of 2D material technology. Applications combining small dimensions, low masses, and high resonant frequencies are new and very interesting for ultra sensitive transducers. The operation of CMUT at high frequencies is easier as the dimensions get smaller. CMUTs also have great potential in

biomedical imaging applications such as real time 3D imaging, high frequency imaging, intravascular and intracardiac ultrasonography (Liu *et al.*, 2004). A CMUT device with mono-layer graphene membrane has been published on cavities of 90 μm in diameter (Chong *et al.*, 2014).

CHAPTER 3

GRAPHENE AND SUSPENDED GRAPHENE: PROPERTIES, SYNTHESIS AND TRANSFER

This chapter will go into more detail about graphene and look at its structure and how it leads to exceptional physical properties. Its structure as well as its historical background will be introduced briefly. After giving some important properties of graphene, mechanical properties of suspended graphene membranes in the literature will be summarized. Moreover, commonly used graphene synthesis methods will be summarized and transfer methods used for fabricating suspended membranes will be presented.

3.1. Graphene: A 2D Material

Two dimensional (2D) topological materials, or atomically thin materials, are defined as crystalline materials consisting of a single layer of atoms. It was assumed that 2D materials can not exist in nature for a long time due to thermal instability when isolated and break apart at finite temperatures (Mermin, 1968) until the first synthesis of graphene from highly oriented pyrolytic graphite (HOPG) (Novoselov *et al.*, 2004) at 2004. The graphene isolation from graphite was realized with breaking weak Van der Waals forces between layers, with an adhesive tape. The first isolated single layer material, graphene, can exist as a free-standing material because the small and strong inter-atomic bonds prevent thermal fluctuations which can create destabilization.

After the existence of mono-layer graphene in free standing state, huge amount of research have been directed to discover its extraordinary properties and isolating other variations of 2D materials from their 3D allotrope which can find applications in wide range of device structures. Three years later, after the first isolation of graphene lying on a support substrate, freely suspended single layer graphene was produced proving 2D crystals are stable even without a support substrate (Meyer *et al.*, 2007)

3.2. Crystal and Band Structure of Graphene

Graphene is the crystalline allotrope of carbon and made up of very tightly bonded carbon atoms organized into a hexagonal (honeycomb) lattice via sp^2 hybridization. Due to its crystal structure, consisting of carbon atoms arranged in a 2D plane, graphene has remarkable band structure. Each carbon atom in graphene has a total of 6 electrons and two of them are in 1s shell while four of them are in 2s and 2p shells. If the arrangement of carbon atoms is in the sp^2 state, three hybrid sp covalent sigma (σ) bonds are formed, leaving one p orbital dangling in the perpendicular direction. Each carbon atom which shares one σ bond is about $a = 1.42 \text{ \AA}$ from its three neighbours, separated by angles of 120° and forms a hexagonal lattice on 2D plane. The fourth bond is a pi (π) bond formed by interactions of unhybridized p orbitals, and oriented in perpendicular direction. These σ and π bands are responsible for most of the extraordinary properties of graphene. Fundamentally, the σ bond gives graphene very superior strength while the π bond correspond to electrical properties of graphene.

3.3. Important Properties of Graphene

As mentioned in the Table.3.1, graphene with an atomic thickness of 0.34 nm has very low 2D mass density (ρ_{2D}) value of $7.7 \times 10^{-7} \text{ kg/m}^2$ and extracted 3D mass density (ρ_{3D}) value of 1350 kg/m^3 (Tsioutsios *et al.*, 2016). Being a transparent electronic component, monolayer graphene has unique levels of light absorption (optical opacity) at $\pi\alpha \approx 2.3 \%$ where α is the fine structure constant, results with optical transmittance of 97.7% for monolayer graphene. In the unstrained state it behaves like a metal with zero band gap and if the strain is applied on it, the electronic structure as well as its resistivity will change and its band gap can reach up to 0.95 eV (Chong *et al.*, 2014).

The experimental observation of the properties of graphene is usually performed while graphene is supported on substrates such as flat SiO_2 , silica or SiC. However, dopant, phonon leakages or carrier leakages caused by underlying substrate mask the intrinsic properties of graphene. That is why extracting the properties of graphene while it is suspended over a trench and not interacting with substrate reveals the results closer to the intrinsic properties. For example, graphene loses its highest charge carrier mobility when it contacts a bulk substrate (Bolotin *et al.*, 2008).

Table 3.1. Important properties of graphene

<u>Property</u>	<u>Value</u>	<u>Reference</u>
Atomic thickness, t	0.34 nm	(Nemes-Incze <i>et al.</i> , 2008)
2D mass density, ρ_{2D}	$7.7 \times 10^7 \text{ kg/m}^2$	(Tsioutsios <i>et al.</i> , 2016)
3D mass density, ρ_{3D}	$1350 \times 10^7 \text{ kg/m}^3$	(Tsioutsios <i>et al.</i> , 2016)
Band gap	0 – 0.95 eV	(Chong <i>et al.</i> , 2014)
Optical Transmittance	97.7 %	(Nair <i>et al.</i> , 2008)

3.4. Mechanical Properties of Graphene and Suspended Graphene

Graphene's mechanical properties can be investigated with many different methods including theoretical calculations and experimental observations. Atomistic modeling (Sakhaee-Pour, 2009), continuum modeling (Atalaya *et al.*, 2008), ab-initio calculations (Wei *et al.*, 2009) etc. are the examples of theoretical calculations. The bulge test, nano indentation, AFM peakforce quantitative nano-mechanical mapping (QNM) analyses are the experimental approaches which can be used for the derivation of graphene's mechanical properties. In this section, mechanical properties of graphene are described.

The σ bonds formed by neighbouring carbon atoms lead to an extremely high in-plane stiffness of graphene. Additionally, graphene's inherent strength is its one of the most remarkable properties, due to the robustness of the covalent carbon-carbon bond (0.142 nm long σ bonds). Frank *et al.* (2007) reported the spring constant of $2 \times 2 \mu\text{m}$ suspended graphene membranes (with 2 to 8 nm in thickness) as 1-5 N/m and the Young's modulus of graphene as 0.5 TPa. Besides, Lee *et al.* (2008) reported the Young's modulus of graphene membranes over 1 to 1.5 μm diameter cavities as 1 TPa. Additionally, intrinsic strength of mono-layer graphene or breaking stress which is the maximum stress that a pristine graphene can withstand just before the atoms are pulled apart was found as 42 Nm^{-1} for a defect free mechanically exfoliated graphene monolayers (Lee *et al.*, 2008).

3.5. Synthesis of Graphene

Graphene as an example of large class of 2D crystals can either be extracted from layered 3D materials (top down approach) or grown with single carbon atoms (bottom up approach). Although, all the methods result in similar feature of sp^2 hexagonal lattice, physical properties of synthesized graphene are not identical. Since the mechanical and electrical characteristics of graphene strongly affects the final device performance, preparation of high quality graphene layer is important. There are many methods for synthesis of graphene with their own constraints and strengths. Each kind of production method gives graphene different properties and that is why production method should be chosen according to desired graphene device properties. A highly crystallized grain with minimized defects and contamination (impurity) are desired for high quality graphene. It is possible to use single crystal graphene layers over a few milli meters and polycrystalline graphene films over meters. Domain (grain) size, doping level, and the number of layers need to be controlled for a successful graphene creation. In this section, two commonly used graphene production methods will introduced by considering graphene quality, possibility of large scale production, and transferability.

3.5.1. Mechanical Exfoliation Method

Mechanical exfoliation technique (also known as scotch-tape method) has been the dominant technique for scientific purposes, and it can be used for fundamental research and for making proof of principle devices. The first successful attempt to obtain single layer graphene was done by Novoselov & Geim group with this technique. As stated in (Castro Neto *et al.*, 2009), the bonding energy between interlayer atoms is about 0.4 eV while the inter-atomic bonding energy is $2.7 - 2.9\text{ eV}$. These weak inter-layers of graphite allow layer to be peeled off by an adhesive medium. In this method, adhesive side of tape is pressed onto the graphite block, e.g., HOPG. The tape is then peeled away with thick layers of graphite attached to it. By repeatedly peeling of the layers on the adhesive tape, all that remains is a structure that resembles graphene in other words exfoliated graphene (EG). For the transfer, the tape containing graphene can be pressed onto a target substrate.

This method results in high structural integrity, high cleanliness and low charge doping, because, during the transfer process, graphene does not encounter any other ma-

material except for ambient contaminations and some from the adhesive tape. Although, mechanical exfoliation technique results with high quality graphene properties (related with graphite block quality) and obtained graphene is monocrystalline, the yield of produced graphene is very low. Graphene flakes up to few multiples of 10 microns in size can be extracted, and their size is determined by the grain size of the graphite.

3.5.2. Chemical Vapour Deposition Method

Chemical vapour deposition (CVD) technique have a principle of the activation of gaseous reactants with the catalyst surface. This activation creates a stable solid deposit over a surface of the substrate. While realizing graphene growth with CVD process, carbon is provided in the gas form and a metal is used both as a substrate and a catalyst. Single crystal, large area, and uniform mono layer or multi layer graphene can be grown on a large number of substrates with CVD technique (Li *et al.*, 2009, 2011). Various refractory metals, such as, Cu, Ni, Ti, Ag, Au have been used for graphene synthesis (Batzill, 2012) since their nonfilled d-shells enable them to absorb carbon during interaction (Seah *et al.*, 2014). Among these transition metals, Cu and Ni are the commonly used ones due to their stability, abundancy, and their easily handled etching process (Mattevi *et al.*, 2011). Besides, the chemical reaction between carbon source and metal layer demands an energy, and that energy can be provided with various sources. While heat is used in thermal CVD, light is used in laser assisted CVD and electric discharge is used in plasma assisted PACVD. Continuous and large scale (up to 100 meter scale) graphene growth has been already achieved (Kobayashi *et al.*, 2013) by using thermal CVD method. The schematic representation of CVD growth of graphene on Cu foil is shown in Figure 3.1. Here, vacuum system, pressure control system, furnace, and mass flow control (MFC) units are shown. MFC unit controls the flow rate of CH₄, H₂, and Ar gases by using standard cubic centimeters per minute (sccm) flow unit.

Growth on Ni is realized by the diffusion of carbon atoms into the bulk (precipitation process) with low pressure environment nearly at $\approx 800^\circ\text{C}$ (Yu *et al.*, 2008). Because the solubility of C atoms in Ni are high and dependent on temperature during cooling down (segregation process) C atoms diffuse out from bulk (Kim, 2015). The thickness of resulting graphene can be controlled by cooling rate. quality and thickness of synthesized graphene depend on thickness and crystallinity of substrate as well as heating and cooling rate of the chamber, process temperature and ratio of gases.

In contrast to Ni, graphene synthesis on Cu is activated through the surface reac-

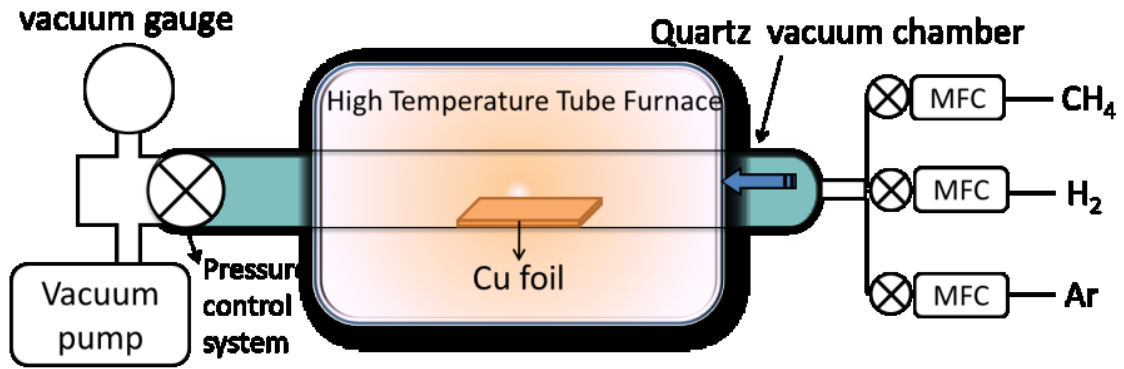


Figure 3.1. Schematic of CVD growth of graphene (source: Kumar and Huei, 2013).

tions because of low solubility of C in the Cu bulk (Li *et al.*, 2009). Graphene synthesis on Cu is independent of cooling temperature and graphene growth on Cu is realized nearly at 1000 °C, which is approximately the uppermost temperature to increase the size of Cu grain boundaries before reaching melting temperature of Cu (1085 °C). Li *et al.* (2009) demonstrated that CVD growth process on Cu catalysts is surface mediated and self-limiting. Due to the difference in the solubility of carbon in these two catalysts, the graphene grown on copper foils results in almost uniform single layer graphene, whereas the growth on nickel results in non-uniform mono and multilayer regions. That is why, while Cu is an appropriate metal for making uniform thickness, large area, mono-layer graphene films, Ni is appropriate metal for multi layer graphene growth.

Figure 3.2 illustrates the growth of graphene on Cu substrates by using CVD. It starts with copper foil and its native oxide layer. This is followed by the reduction of oxide layer and increase of grain boundary sizes at high temperature annealing. After that illustrates the exposure of the Cu foil with carbon source at 1000 °C leading to the nucleation of graphene islands (Kumar and Huei, 2013). Additionally, carbon prefers to precipitate out through the defect sides of the bulk which result in thicker graphitic layers on them (Graph, 2013), as shown in Figure 3.3.

3.6. Transfer of CVD Synthesized Graphene on Target Substrates

Graphene synthesis can be realized with different methods and for each growth method transfer is possible with different approaches. Because, the CVD growth of

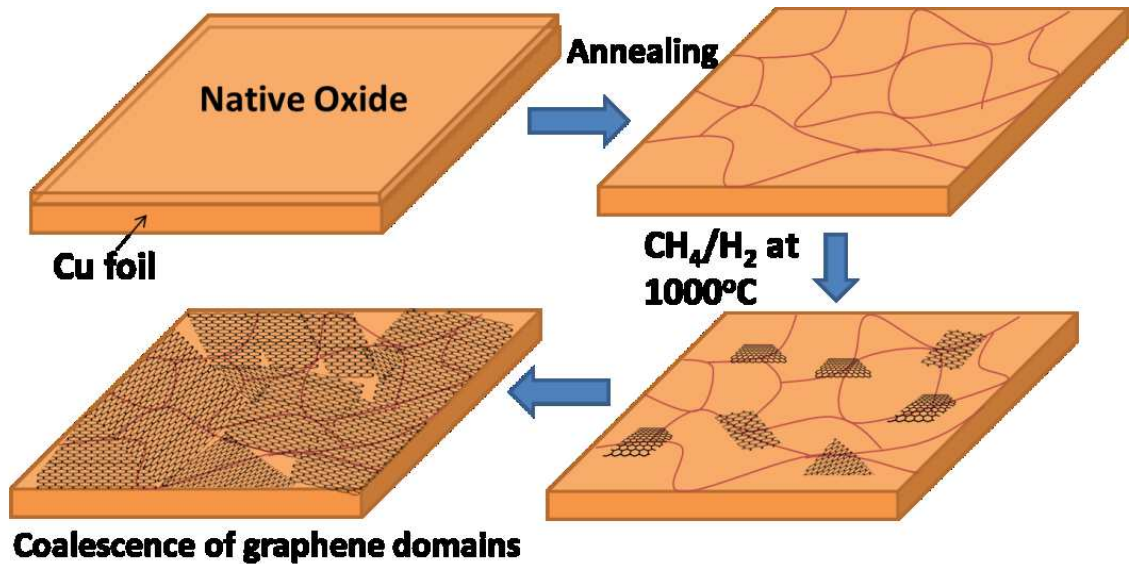


Figure 3.2. Schematic of graphene synthesis on Cu foil (source: Kumar and Huei, 2013).

graphene has chosen as appropriate method for this thesis study the transfer of CVD synthesized graphene from metal seed layer to cavity structures will be detailed in the following.

CVD grown graphene results with a catalyst substrate and large area, polycrystalline graphene layer on it. After the growth, graphene layer on catalyst substrate can be transferred on to desired substrates. Thermal treatment allows the transferred graphene films attach strongly to almost any material via van der Waals interactions (Reina *et al.*, 2009). The transfer process should be optimized with the objectives of minimizing damage to graphene. Furthermore, the transfer of graphene on substrates with micro scale cavities is more challenging, because, the process can result in membrane collapse. For a CVD grown graphene films, transfer approaches can be categorized from two different aspects. Firstly, the transfer process can be categorized according to interaction between the graphene layer and the substrate. If the interaction occurs in a solution such as deionized (DI) water, this process can be named as wet transfer and if not, dry transfer. Secondly, the process can be categorized according to existence of supportive layer during transfer. If transfer is realized without any additional polymer layer to support graphene during transfer, the method is named as polymer free transfer. On the other hand, if the transfer is realized with the support of polymer layer, the process is named as transfer via support. In all approaches and methods, the removal of the catalyst substrate is realized with chemical etching or delamination methods (Liechti *et al.*, 2015).

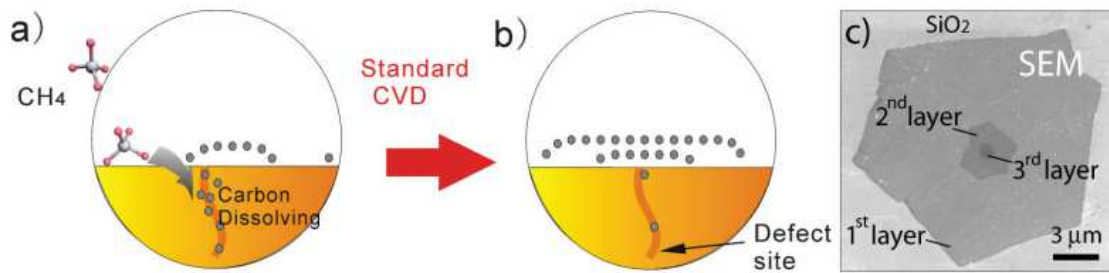


Figure 3.3. Illustration of graphene synthesis on defects side of the foil, (a) dissolving of carbon atoms inside the defect sides at high temperatures, (b) the dissolved carbon atoms forms graphene layers during cooling down process, (c) SEM image showing the graphene layer number differences around the defect sides, (source: Graph, 2013).

3.6.1. Transfer Approach 1: According to the Interaction Between Graphene and Target Substrate

This classification depends on whether any liquid is involved when the graphene layer interacts with target substrate. If the graphene is floating in a solution (like DI water or an etchant) during the interaction between graphene and target substrate, the method can be called as wet transfer. Fishing method can be an example of wet transfer method. On the other hand, during the dry transfer process, a CVD grown graphene with supportive layer interacts with the target substrate in a liquid-free environment. As shown in Figure 3.4 both the wet and the dry techniques include wet etching of metal foil in an etchant. If the target substrate includes shallow wells dry transfer is appropriate because it is required to avoid trapping liquids in the wells. But, for the flat or perforated substrates both wet and dry transfer techniques are applicable (Suk *et al.*, 2011).

3.6.2. Transfer Approach 2: According to the Additional Support Layer

The transfer process can be categorized according to existence of supportive layer during the transfer. If the transfer is realized without any additional polymer layer to support the graphene, the method is named as polymer free (direct) transfer. On the other

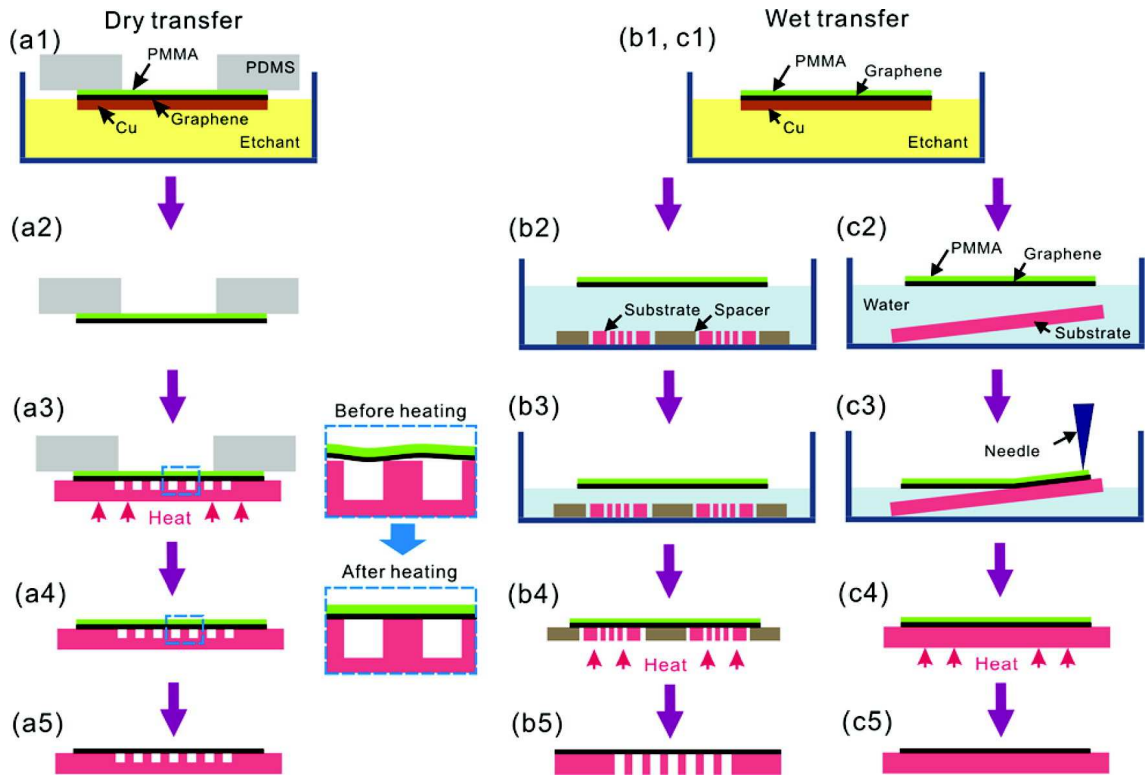


Figure 3.4. Schematic of wet and dry transfer procedures (a) dry transfer onto cavities, wet transfer onto (b) perforated and (c) flat substrates. Dashed lines are for magnified images (source: Suk *et al.*, 2011).

hand, if the transfer is realized with a supportive polymer layer, the process is transfer via support (also named as standard transfer).

Direct transfer of graphene on to a target substrate can use the capillary action of solvent droplets. Regan *et al.* (2010) used isopropyl alcohol (IPA) as an adhesion promoter. They placed amorphous carbon transmission electron microscopy (TEM) grid on to a graphene layer on copper foil and dropped IPA. As the IPA evaporates, surface tension draws the graphene and grid together into contact (adhesion and suspension of graphene on a TEM grid). The suspended membranes were $1.2 \mu\text{m}$ in diameter. Moreover, Ledwosinska *et al.* (2012) reported an organic free method for creation suspended graphene membranes over 10 to $20 \mu\text{m}$ apertures. In the reported method, suspended membranes were obtained with isotropic etching of underlying Cu foil with 0.1 M of $(\text{NH}_4)_2\text{S}_2\text{O}_8$ etchant.

Standard transfer method is one of the most widely used method for transfer of CVD grown graphene and based on coating a polymer material on a graphene metal substrate as support layer. The illustration comparing standard and direct transfer methods

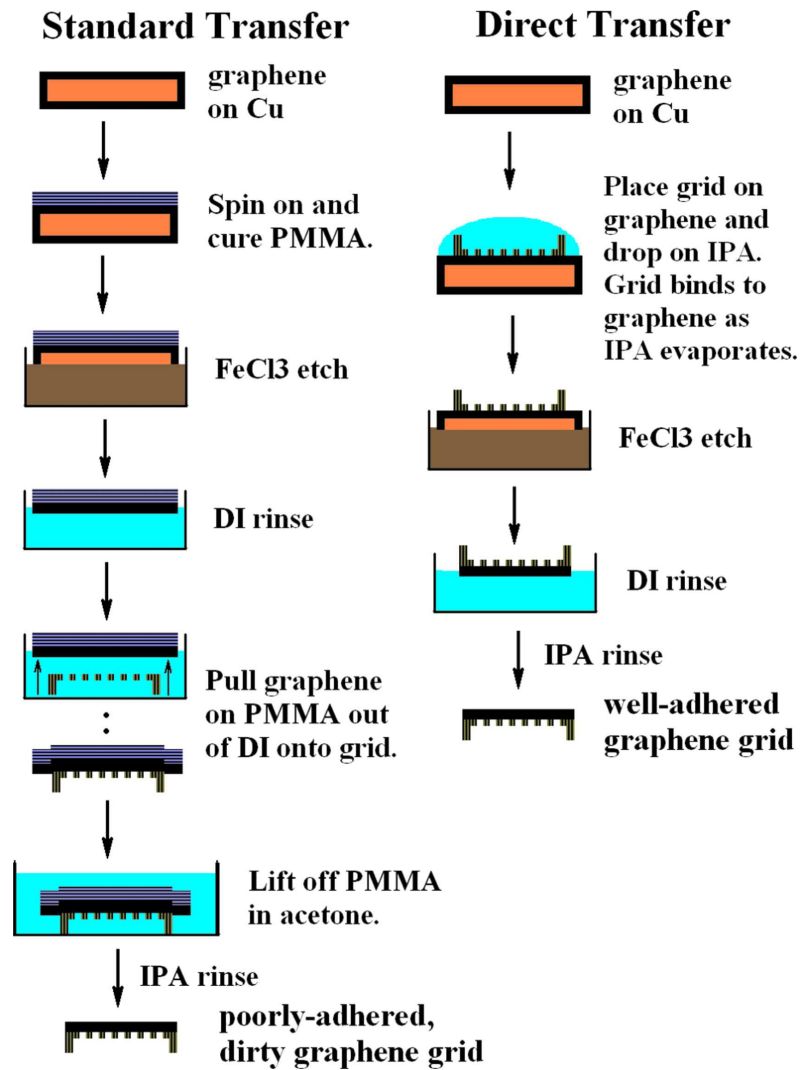


Figure 3.5. Schematic of standard (left) and direct (right) transfer methods (source: Regan *et al.*, 2010).

is presented in Figure 3.5. In this method, the carrier polymer film can be PMMA (Suk *et al.*, 2011), photoresist (Polat *et al.*, 2015), polydimethylsiloxane (PDMS) stamp (Hallam *et al.*, 2015), thermal release tape (Caldwell *et al.*, 2010), epoxy (Liechti *et al.*, 2015), anthracene layer (Yulaev *et al.*, 2016), etc. After the transfer, support carrier polymer film can be dissolved with alternative ways. If the carrier film is PMMA or photoresist dissolution can be done with chemical etching in organic solvents like acetone. If it is a PDMS stamp, mechanical detachment can be used. And if the carrier film is a thermal release tape, PMMA or anthracene, thermal annealing in vacuum can be applied in order to remove the carrier film after transfer.

Figures 3.6 and 3.7 are examples of this transfer method with PMMA as a support

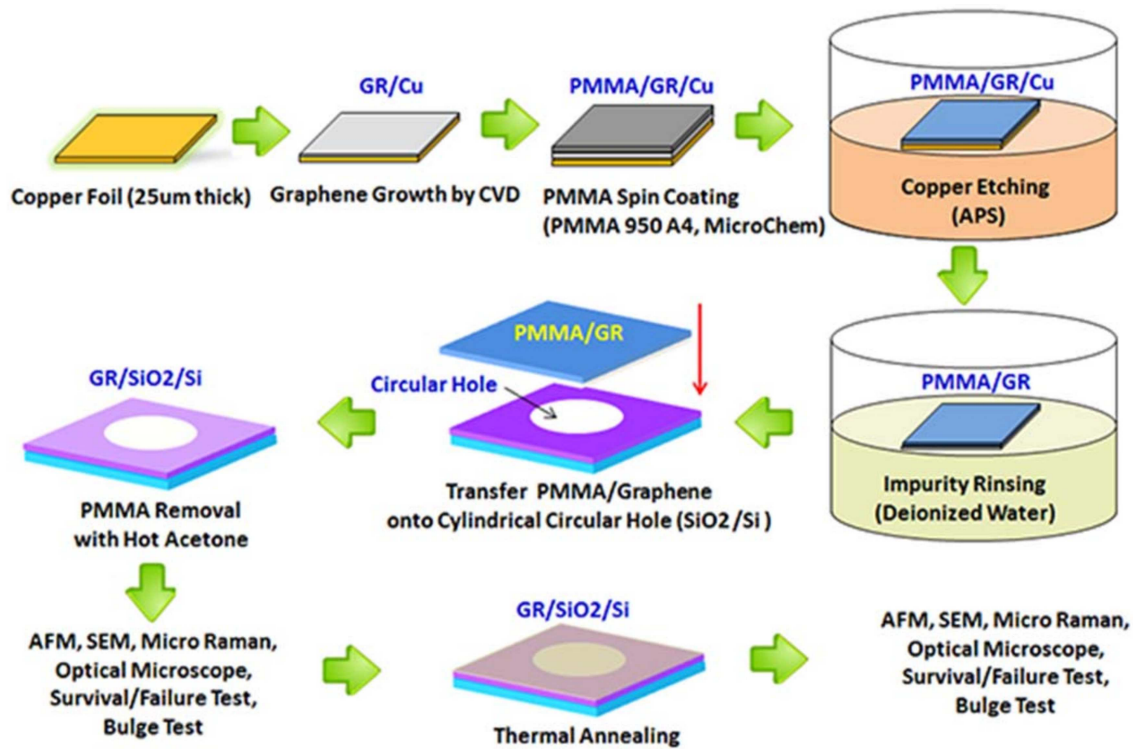


Figure 3.6. Transfer of graphene on SiO₂ substrates with cavities (10 and 110 μm in diameter) with PMMA support layer (source: Hwangbo *et al.*, 2014).

layer. Graphene grown by using the CVD on polycrystalline copper (Cu) was transferred via PMMA material onto SiO₂ substrate with a cylindrical holes. In the study presented in Figure 3.6, hole diameters are changing between 10 and 110 μm . Additionally, after the transfer of graphene on the cavity structure, the PMMA removal was realized by using hot acetone and the thermal treatment. Membranes were thermally annealed for 2 hours in 1 Torr pressure with 500 sccm Ar flow at 250 and 350 $^{\circ}\text{C}$ (Hwangbo *et al.*, 2014). Moreover, in the study of Lee *et al.* (2014), suspended graphene membranes over predefined cavities were fabricated (Figure 3.7). By scooping up the PMMA/graphene immersed in DI water on to the perforated SiO₂ substrate the transfer was realized. The samples were dried for approximately 6 hours at room temperature after baking the sample in an oven at 80 $^{\circ}\text{C}$ to improve the adhesion between the graphene and the substrate. Finally, the free standing graphene was obtained by removing the PMMA layer by using 3 different wet etching process named as dipping, substituting and inverted floating methods. The methods used as removal of PMMA material is shown in Figure 3.8. In conventional dipping methods, acetone etchant is used for the removal of PMMA. But, in the substituting method, acetone is slowly mixed with methoxynonafluorobutane. In the inverted floating

method, acetone only contacts with the PMMA, preventing the interaction of the etchant inside the holes. Because, the chemical etching and drying processes for the PMMA induce a stiction between the graphene and the vertical wall of the hole due to van der Waals and capillary forces, and this stiction can result in broken membranes (Song *et al.*, 2012). While with dipping and substituting steps, graphene membranes up to $30\ \mu\text{m}$ was achieved with inverted floating method, membranes up to a half mm scale was obtained.

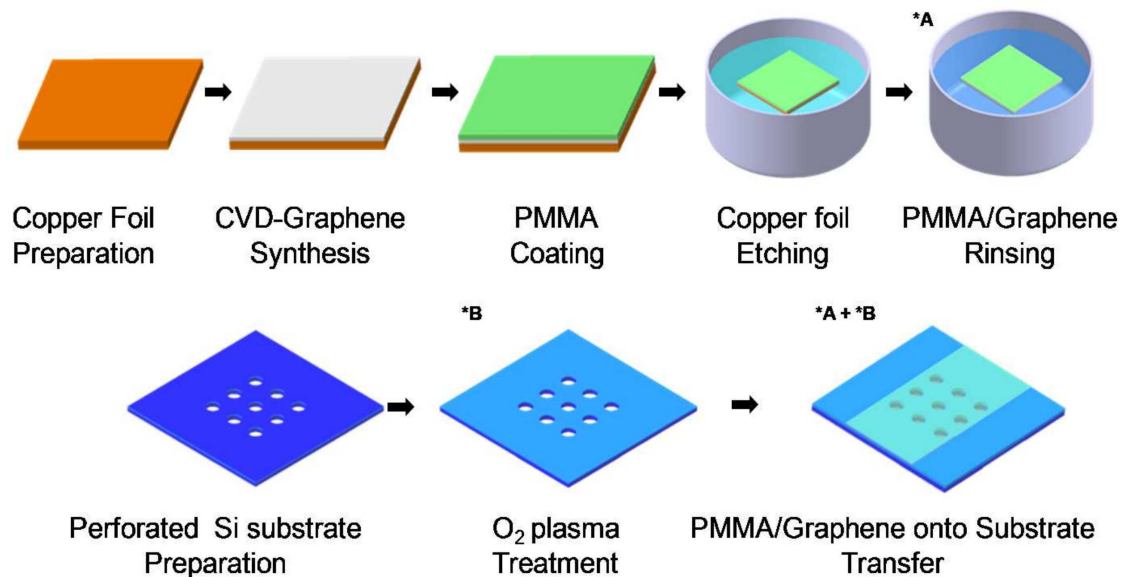


Figure 3.7. Transfer of graphene on SiO_2 substrates with cavities with PMMA support layer (source: Lee *et al.*, 2014).

Additionally, Berger *et al.* (2017) demonstrated a transfer technique (Figure 3.9) for CVD synthesized graphene on copper foils for suspended graphene membranes supported by a PMMA layer (thickness of $18\ \text{nm}$ to $235\ \text{nm}$). Micro membranes up to $30\ \mu\text{m}$ were fabricated. Here, the transfer process begins with flattening step. In order to flatten the graphene, graphene with PMMA layer is transferred on to a plasma cleaned flat Si/ SiO_2 substrate with fishing method. Then, the tape supported polymer/graphene membrane is transferred on to the patterned Si/ SiO_2 substrate.

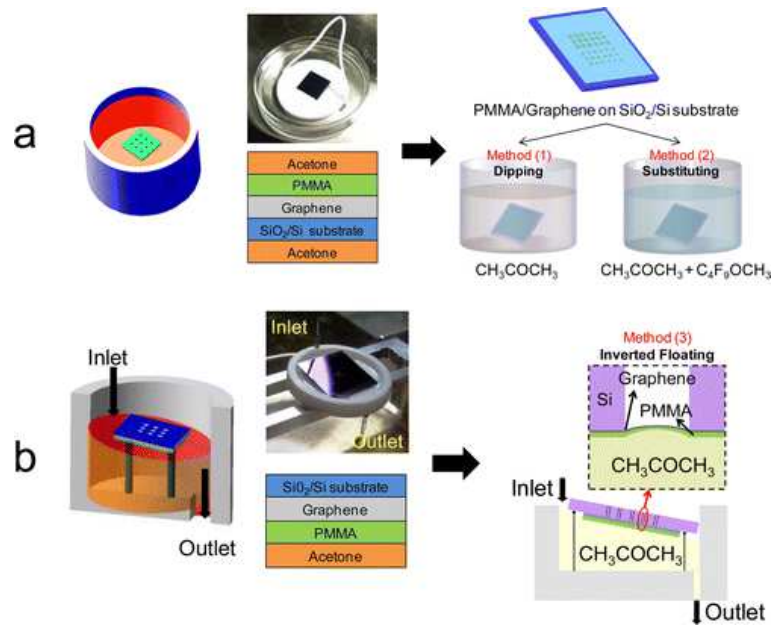


Figure 3.8. Methods for PMMA removal for fabricating free standing CVD graphene, (a) conventional (b) inverted floating method (source: Lee *et al.*, 2014).

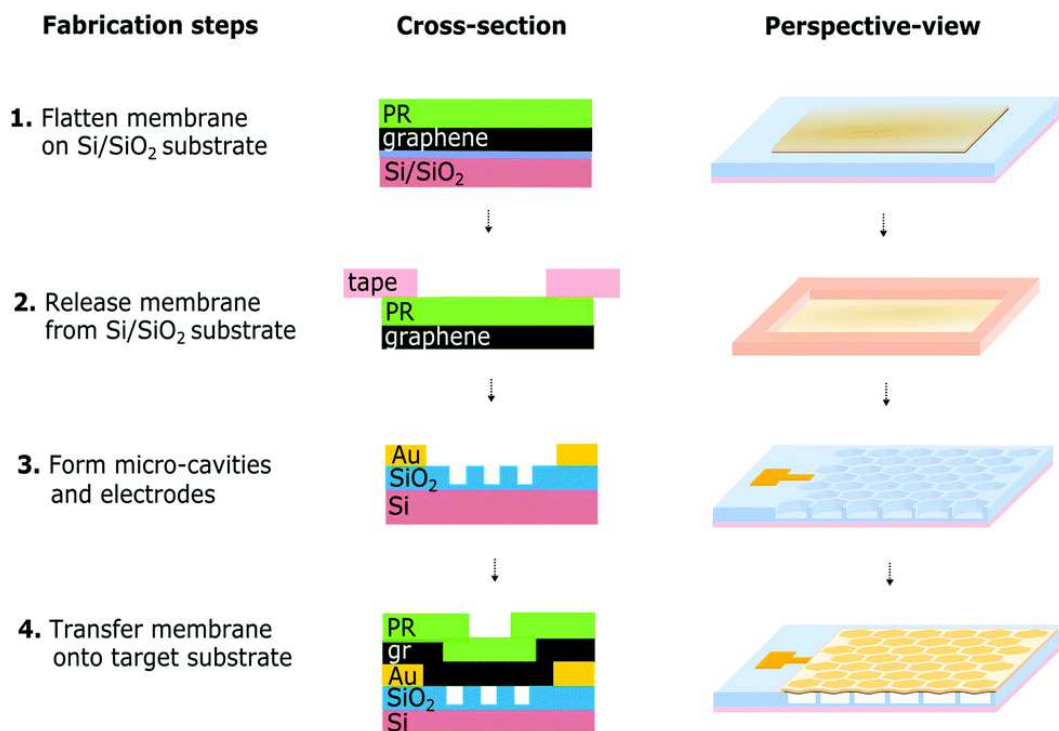


Figure 3.9. Schematic presenting the fabrication of free standing CVD graphene with PMMA material (source: Berger *et al.*, 2017).

CHAPTER 4

CHARACTERIZATION TECHNIQUES

In this chapter, characterization methods for graphene films and suspended graphene membranes performed with optical microscope, scanning electron microscope (SEM), Raman spectroscopy and atomic force microscopy (AFM) are presented with a brief overview of each method in the following sections. Without any equipment it is also possible to distinguish mono layer graphene transferred on to a 90 nm or 300 nm thermal oxide films on Si layer with a trained eye (Blake *et al.*, 2007).

4.1. Optical Microscopy

The preliminary characterization of the suspended membranes can be realized by using visible light microscope. Under the white light illumination, the visibility of graphene by interference effect is maximized at an oxide thickness of 90 nm and 300 nm when graphene transferred onto SiO₂ substrates, see Figure 4.1. Besides, with blue narrow-pass filter, mono-layer graphene is visible on almost any thin film (Blake *et al.*, 2007).

4.2. Scanning Electron Microscopy

Scanning electron microscopy (SEM) is a non-contact, mostly non-destructive and efficient tool for fast imaging. SEM has been intensively applied to image and characterize features of graphene in micro and nano scales. By using this technique finding the yield of suspended graphene layers as well as observing low scale structural defects like, grain shapes, wrinkles, tears, folds (Lee, 2015; Lee *et al.*, 2015) is possible. Different kind of detectors can collect data from different penetration depths of sample electron interaction. Additionally, low accelerating voltage can lead to smaller penetration depth. That is why, for morphological characterization of graphene (2D structure just laying on the sample surface) low accelerating voltage and backscattering electron detector can be used. Moreover, folding graphene lines, in other way, dark lines in an image can be in-

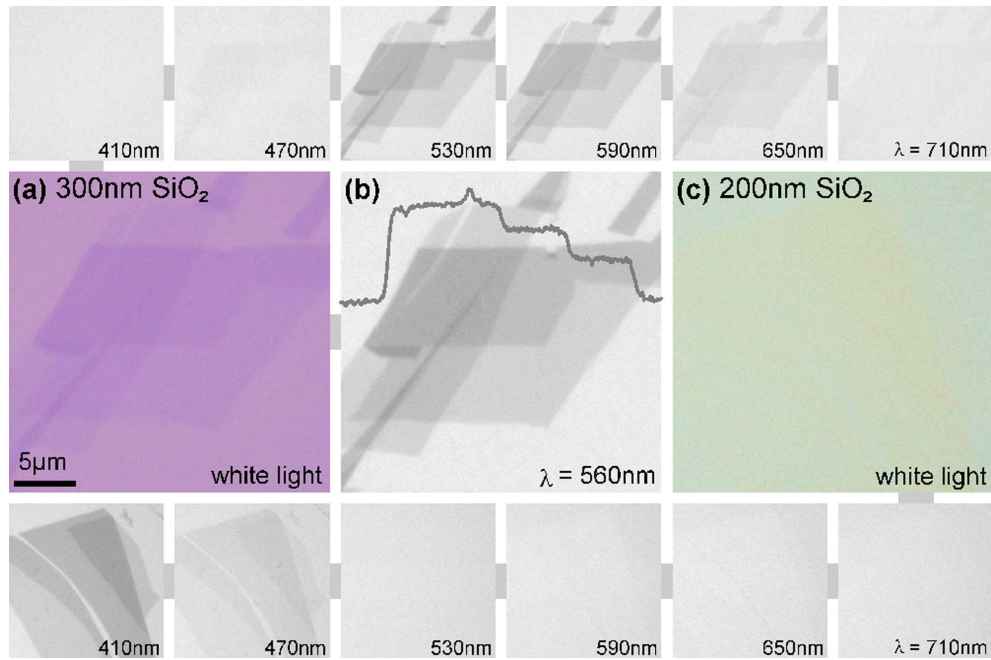


Figure 4.1. Optical microscope images of graphene layers on SiO_2/Si . Different thicknesses and light wavelengths results in different optical contrast and the contrast corresponds to layer number differences. Image sizes are $25 \times 25 \mu m$ (source: Blake *et al.*, 2007).

investigated by the secondary electron detector. While the dark lines corresponds to folded graphene layers, bright lines indicates the information about wrinkles (Lee *et al.*, 2015). In an SEM image the difference between mono layer, few layer and multi layer graphene can be investigated by using contrast and brightness difference. The reason of this relies on the transparency of graphene to high energy electrons. Backscattered and secondary electrons are generated from the Cu substrate. These electrons need to pass through the graphene layer and collected by the SEM detectors. During that process graphene blocks some returning electrons and as the number of layers increase the blocking will increase which results in brightness of image. As mentioned in (Hiura *et al.*, 2010), by calibrating brightness, number of layers of graphene can extracted by using SEM.

4.3. Raman Spectroscopy

Raman spectroscopy is an optical characterization technique and used to characterize the phonon spectrum of sp^2 and sp^3 hybridized carbon atoms (graphene and other

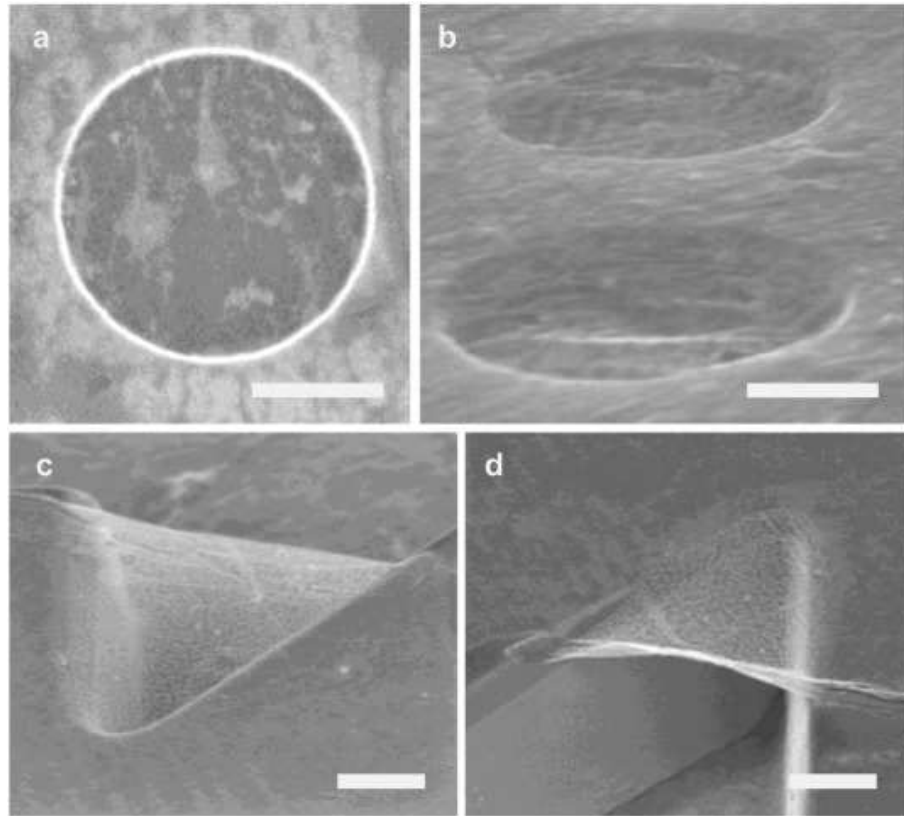


Figure 4.2. SEM images of circular drumhead graphene from top view (a) and 45° tilted (b) views. (c) and (d) show graphene over triangular trenches with 52° tilted view. All the graphene layers are on 290 nm SiO_2 on Si substrate. All scale bars are $1\ \mu\text{m}$ (source: Lee *et al.*, 2015).

graphitic materials). Raman spectrum of graphene is used for determining the number of graphene layers (thickness), stacking order, strain, density of defects and impurities by examining the peak positions, the peak shapes and the relative intensities of the peaks (Cooper *et al.*, 2011; Ferrari and Basko, 2013). The dispersion relation of graphene gives information about phonon modes as a function of frequency (Falkovsky, 2007). The spectrum of graphene occur in the region between 1250 cm^{-1} and 3400 cm^{-1} and include three main peaks. The Raman spectrum for mono, bi, and few layer graphene and spectrum for highly oriented pyrolytic graphite (HOPG) under 514 nm laser excitation are given in Figure 4.3.

- D Band ($\approx 1350\text{ cm}^{-1}$) D band, so called double resonant raman scattering, is the defect peak results from disorders in graphene lattice. D peak is around 1350 cm^{-1} with a 514 nm laser excitation. This position is also changing with laser excitation frequency. If the graphene layers are highly ordered (pristine), it is not possible to

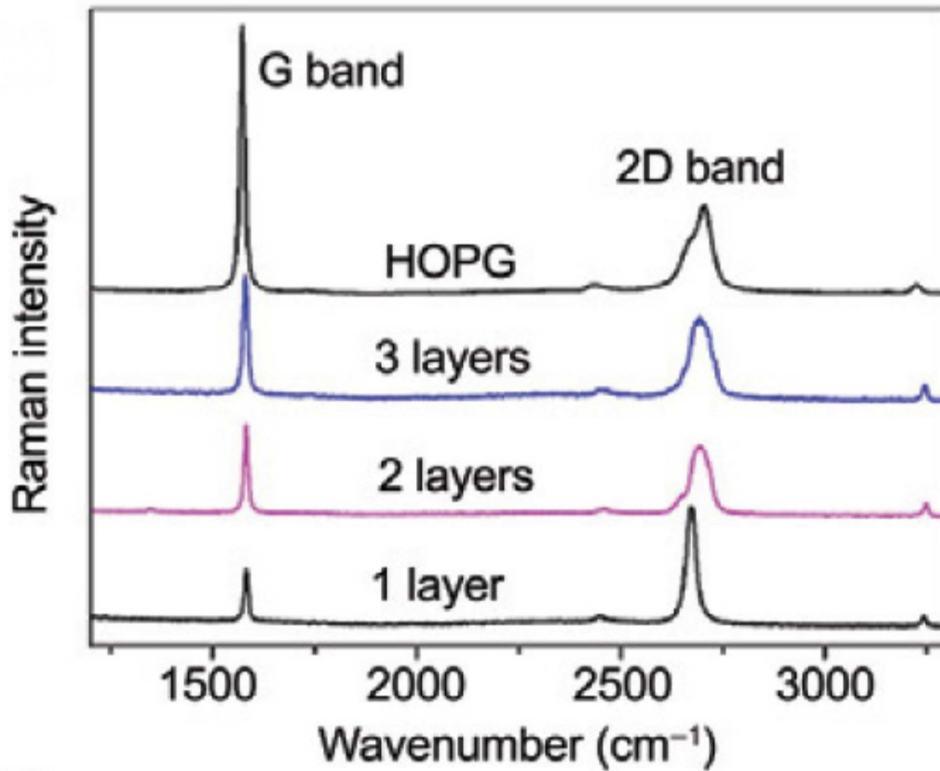


Figure 4.3. Raman spectra for mono, bi, few layer graphene and graphite (HOPG) (source: Cantarero, 2015).

observe peak.

- G Band ($\approx 1580 \text{ cm}^{-1}$) The G band, as being the most prominent behavior of graphitic materials, induced by in plane vibrations of sp^2 carbon atoms. This peak corresponds to E_{2G} vibrational mode in first order Raman scattering process and found at around 1580 cm^{-1} . The G band is single resonant and sensitive to the strain and doping (Beams *et al.*, 2015).
- 2D Band ($\approx 2700 \text{ cm}^{-1}$) The 2D band appears at around 2700 cm^{-1} for a 514 nm laser excitement. Like D band, 2D band is also resulted from double resonance scattering but does not need any defect to occur. Ferrari and Basko (2013) demonstrated that single layer graphene has a sharp, symmetric Lorentzian peak and the peak intensity ratio of 2D peak to D peak (I_{2D}/I_G) is nearly equal to 2. Additionally, for bilayer graphene this ratio is nearly equal to 1 and for multilayer graphene the ratio of 2D mode and G mode of the spectrum is observed as having a value smaller than 1.

4.4. Atomic Force Microscopy

To obtain the topological characteristics of graphene membranes, tapping-mode AFM can be used. Moreover, with force-distance measurements, the stiffness values of membranes can be determined. In the study of Lee *et al.* (2008), shown in Figure 4.4, AFM nanoindentation technique is used to measure the mechanical properties of mono-layer graphene membranes.

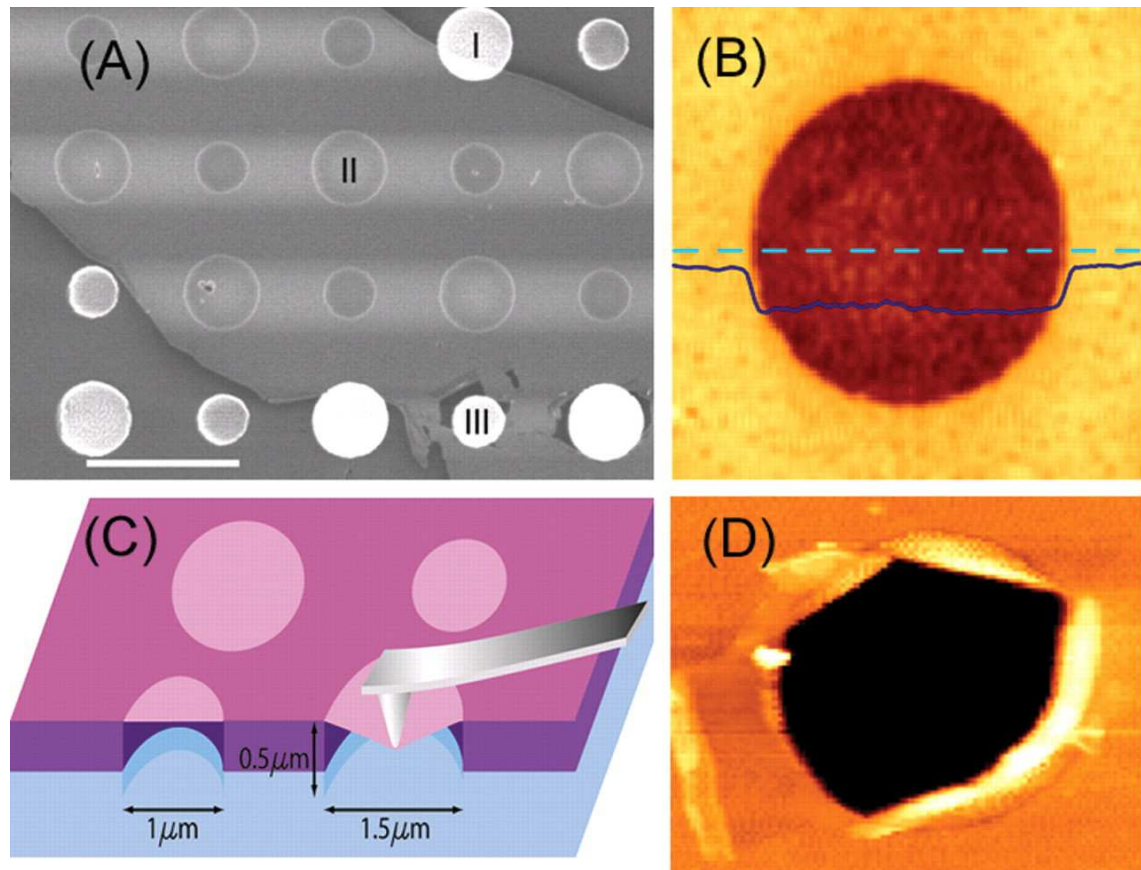


Figure 4.4. (a) SEM image of membranes over cavities changing between 1 and 1.5 μm in diameter with scale bar of 3 μm . I is partially covered, II is fully covered and III is fractured graphene. (b) noncontact AFM image of suspended graphene. Solid line is the height profile (2.5 nm) along the dashed line. (c) schematic showing the AFM nanoindentation technique. (d) noncontact AFM image of a fractured graphene membrane (source: Lee *et al.*, 2008).

CHAPTER 5

TRANSFER APPROACHES TO FABRICATE GRAPHENE MICRO MEMBRANES

This thesis focuses on the transfer of graphene on to the cavity structures to fabricate suspended micro membranes. Different support materials are used for the graphene transfer process. Fabrication includes these main steps: atmospheric pressure chemical vapour deposition (APCVD) synthesis of graphene, fabrication of substrates with cavities, and the transfer of APCVD grown graphene on to the substrates with cavities. The characterization of fabricated structures are done by using optical microscope, SEM, Raman spectroscopy, and AFM.

5.1. APCVD Synthesis of Graphene

The graphene synthesis is realized by using a home-built APCVD system. Mono and few-layer graphene growth is realized on Cu foils. The multi-layer graphene on Ni foil is obtained from a commercial company (Graphene Supermarket). The graphene thickness on the Ni foil is also confirmed with AFM height profile analysis and found to be between 500 and 800 *nm*. The samples are characterized by using optical microscope and Raman spectroscopy to optimize the CVD growth parameters and homogeneity of transferred graphene.

Cu foils (Alfa Aesar, 99.8 % purity, 25 μm in thickness) is used to form graphene. Prior to the CVD growth, $\approx 3 \times 3$ *mm* Cu foils are waited in Nitric acid : DI water solution (1:11) for 60 seconds in order to decrease copper foil roughness and to remove native oxide layer. Right after the cleaning and drying procedures, the copper foils on a quartz sample holder are loaded into a quartz tube in the APCVD setup. APCVD setup used in this study is presented in Figure 5.1. CVD setup mainly consists of high temperature furnace, thermocouple temperature sensor, chamber pressure controller, gas sources and gas flow controller unit.

The graphene growth on Cu foils in the chamber of APCVD setup follows four main steps which can be stated as follows: Ramping up the temperature, annealing the

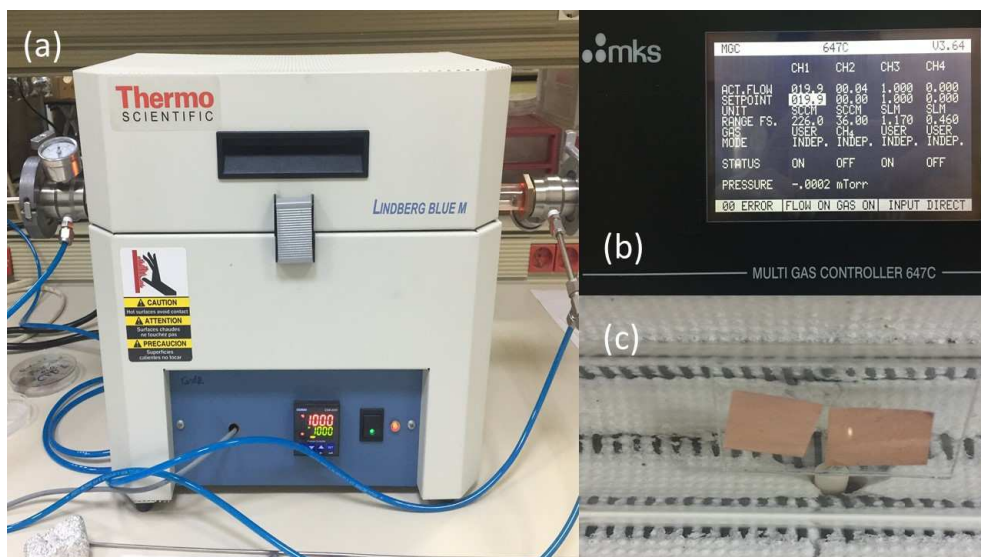


Figure 5.1. APCVD growth unit (a) Lindberg Blue oven from Thermo Scientific Instruments (b) gas flow controller unit (c) Cu foils inside the growth chamber.

Cu foils, carbon source introduction to the growth chamber and cooling down process. In the first step, pre-cleaned $\sim 3 \times 3$ mm sliced copper foils are inserted in APCVD growth chamber, followed by ramping up the room temperature to 1000°C in 33 minutes. Meanwhile, Argon (Ar) and Hydrogen (H_2) gases are introduced to the growth tube in vacuum environment. Controlled flow rates of Argon (Ar) and Hydrogen (H_2) gases are used as 1000 and 20 *sccm*, respectively. When the furnace temperature reached to 1000°C , annealing step of Cu foils is started. In this process, the Cu foils are waited for 60 minutes in Ar and H_2 environment for stabilizing the temperature of substrates. Moreover, annealing process cleans the surface of Cu foils and generates larger Cu grain boundaries on the surface (Lee *et al.*, 2015). After this process, methane (CH_4) gas is introduced as a carbon source. Synthesis of mono-layer and few-layer graphene is realized with changing the duration and the flow rate of the CH_4 material. The cooling down step is done by opening the furnace cover. During the cooling down step the same composition of Ar and H_2 gases is maintained.

Table 5.1 presents the growth parameters to synthesize mono and few layer graphene using APCVD growth technique used in this study. Synthesis of mono-layer graphene is realized by using 5 *sccm* of CH_4 gas for 2 minutes while 10 *sccm* of CH_4 gas is introduced to the chamber for few-layer graphene growth for 20 minutes. The diagram of mono-layer graphene growth with CVD technique is shown in Figure 5.2.

Table 5.1. Parameters used for APCVD graphene synthesis

Graphene Property	Growth Temperature (°C)	Ar		H ₂		CH ₄	
		duration (min)	flow rate (sccm)	duration (min)	flow rate (sccm)	duration (min)	flow rate (sccm)
Mono layer	1000	120	1000	120	20	2	5
Multi layer	1000	120	1000	120	20	20	10

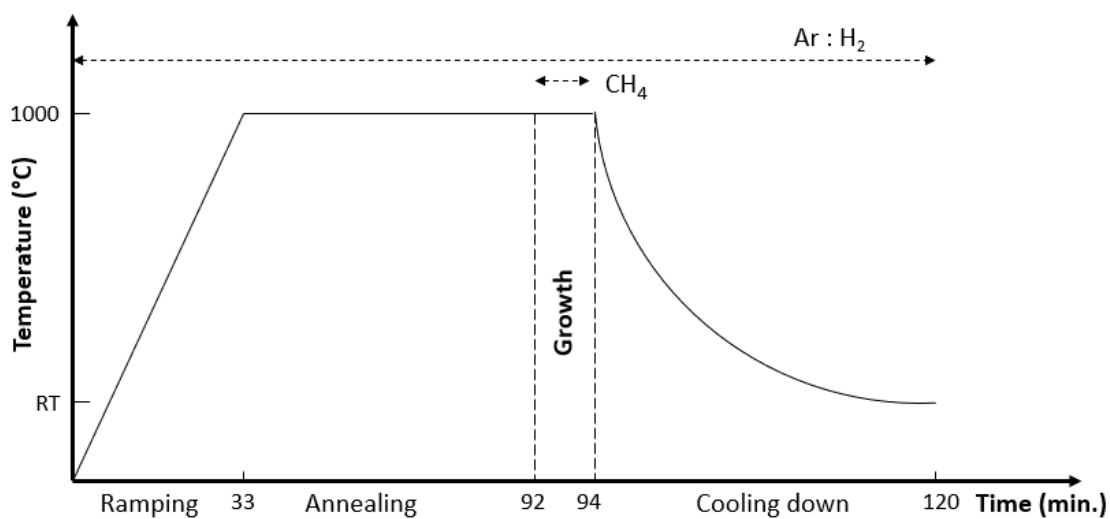


Figure 5.2. Temperature-Time graph presenting the mono-layer graphene growth steps with APCVD technique on Cu foil.

5.1.1. Transfer of APCVD Grown Graphene on Flat Substrates

After the CVD growth, the resulting material is graphene on both faces of Cu foil. For that reason, O₂ plasma treatment is applied to the bottom face of Cu foil to remove graphene. Suspended graphene membranes can be fabricated by etching Cu foils in a patterned way using lithography techniques (Alemán *et al.*, 2010) but, if the resulting device do not include Cu, the removal of Cu foil is needed. Moreover, it is not possible to transfer graphene from copper foil to the target substrate directly because the adhesion energy between Cu foil and graphene is relatively high, 6 J/m^2 , (Na *et al.*, 2015). Before the transfer, liquid etching of copper foil is needed to free the CVD graphene and let the graphene to adhere on to the substrate of interest. On the other hand, without a support material, the graphene layer is too slim to remove from the etchant without wrinkling. That is why the transfer needs to be done by using a support material. All the transfer techniques used in this study is performed by using support layer on the graphene.

Depending on the transfer medium, the transfer can be classified as dry and wet. In the dry transfer, CVD-graphene is transferred on to the flat Si substrate with 300 nm oxide on top of it using S1813 type photoresist material. Photoresist liquid is dropped on the surface of the graphene/copper sample. After the sample is waited for 12 hours in 70 °C hot oven to obtain the support film, the copper is etched away with 1M ferric chloride FeCl₃ in DI water. Once the Cu foil is completely etched away, the graphene with support photoresist is waited in HCl:DI water solution prepared with a volume ratio of 1:3 to rinse off any impurity and residue of FeCl₃ and then transferred to a flat beaker of deionized water. The rinsing processes in DI water are repeated several times. Then, the sample is dried by using Ni flow and transferred on to the SiO₂/Si substrate. After the transfer, the sample is waited on hot plate for 45 seconds firstly at 90 °C to create adhesion between graphene and SiO₂ and secondly 45 seconds at 140 °C in order to liquidize the photoresist. Next the liquified photoresist is removed from grp/SiO₂/Si sample surface by using acetone solution. The acetone residues are cleaned by waiting the sample in the isopropyl alcohol and DI water. The prepared samples are examined by an optical microscope and with Raman spectroscopy analysis. Optical microscope image of the transferred graphene on flat substrate is shown in Figure 5.3 (a).

In the wet transfer (fishing) method, the graphene on Cu foil is covered with PMMA material with spin coating technique (4000 rpm for 45 seconds). After the coating, the sample is waited for 12 hour at room temperature to solidify the PMMA. Then, the Cu foil is etched away with 1M ferric chloride (FeCl₃) in DI water. After the Cu foil

is completely etched away, the solution (FeCl_3) is replaced with HCl :DI water solution prepared with volume ratio of 1:3 to rinse off any impurity and residue of FeCl_3 . Next, the HCl :DI solution is replaced with DI water by using pipettes. While the PMMA on graphene is floating on the DI water, the graphene and the PMMA is scooped out with pre-cleaned SiO_2/Si sample. Then the $\text{SiO}_2/\text{Si}/\text{grp}/\text{PMMA}$ structure is left to dry. After adhesion of graphene to the substrate at room temperature, the PMMA is removed with acetone. The optical microscope image of the transferred graphene on a flat substrate is given in Figure 5.3 (b).

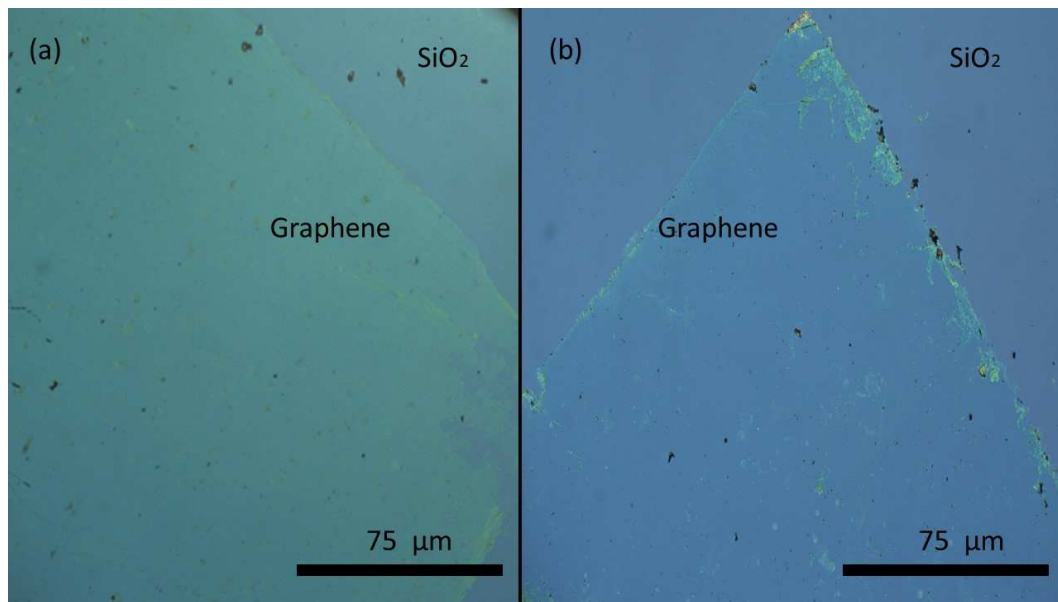


Figure 5.3. Optical microscope images of graphene after transferred on flat SiO_2 samples (a) transferred via dry transfer approach with photoresist as support material, (b) transferred via wet transfer (fishing) approach with PMMA as a support material.

The Raman analyses of transferred graphene layers are given in Figure 5.4 and Figure 5.5, respectively. Raman spectra are collected by a home-made Raman setup. A 514 nm laser is focused by a 100x optical microscope. Before signal acquisition, the system is calibrated by setting the silicon transverse optical peak to $\approx 521 \text{ cm}^{-1}$. The graphene layer number determination can be done by Raman peak ratios and full width at half maximum (FWHM) value of its 2D mode (Ferrari and Basko, 2013). For a monolayer graphene, the ratio of 2D to G mode is approximately 2. While, for bilayer graphene this ratio is nearly equal to 1 and for multilayer graphene the ratio of 2D to G mode of the spectrum is smaller than 1.

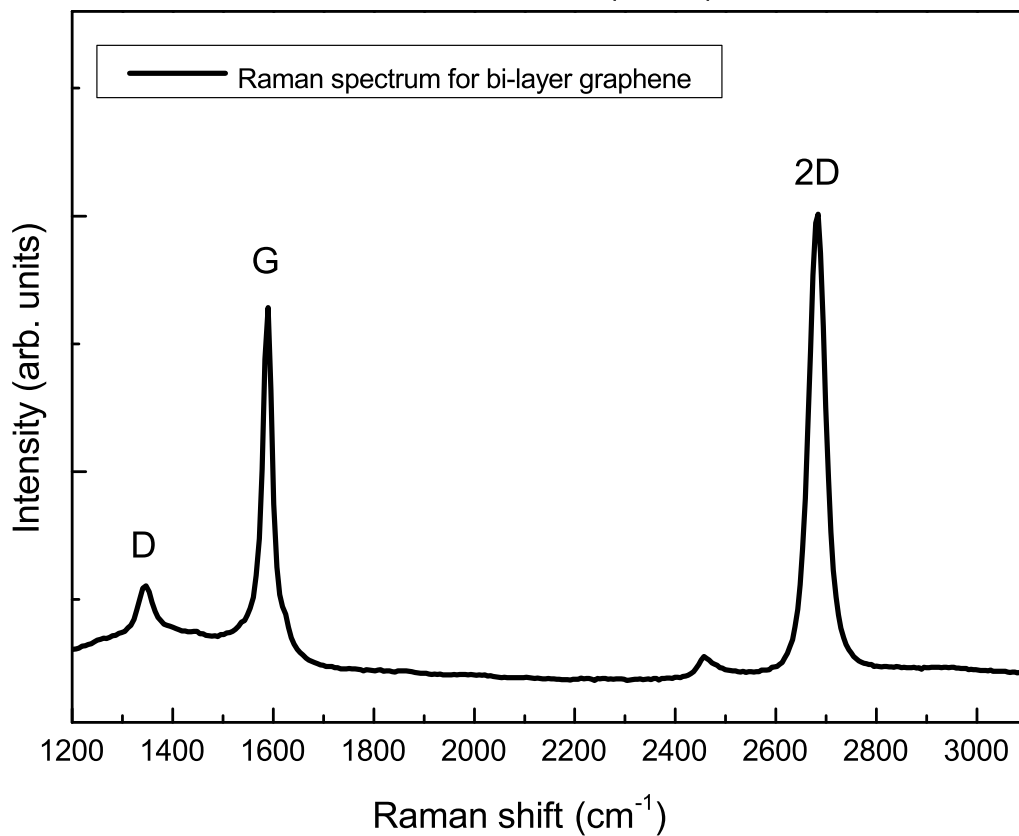
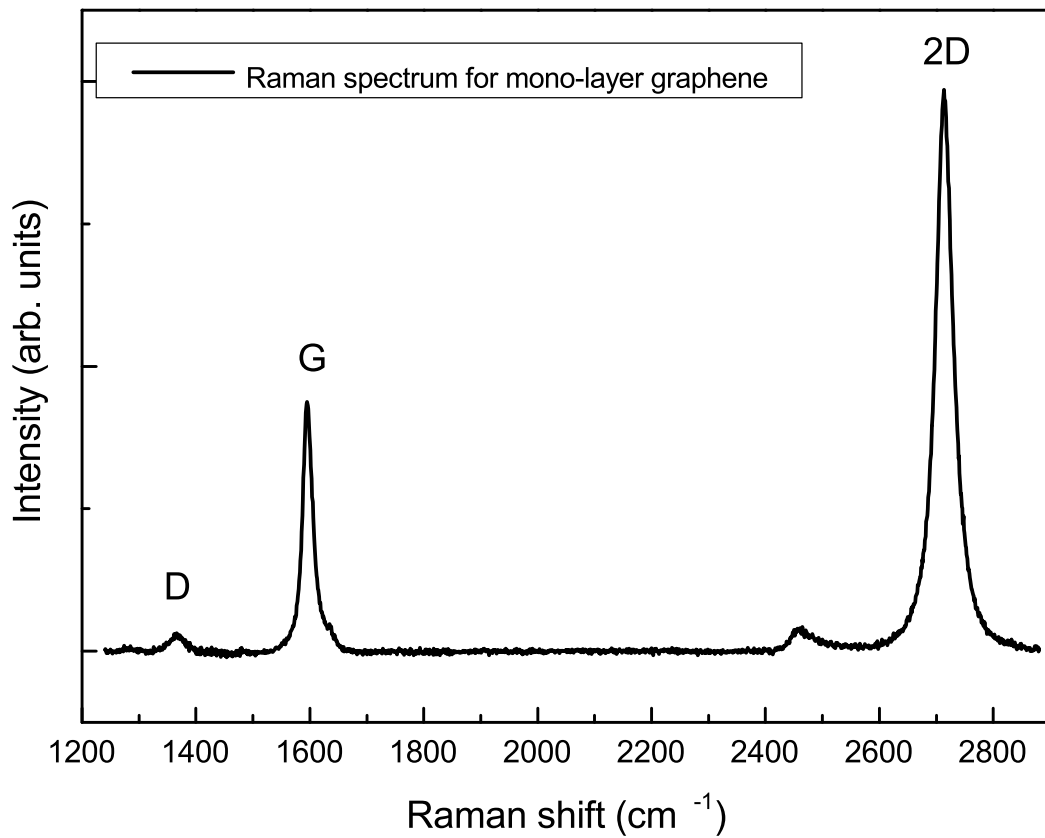


Figure 5.4. Mono and bi-layer graphene Raman spectrum.

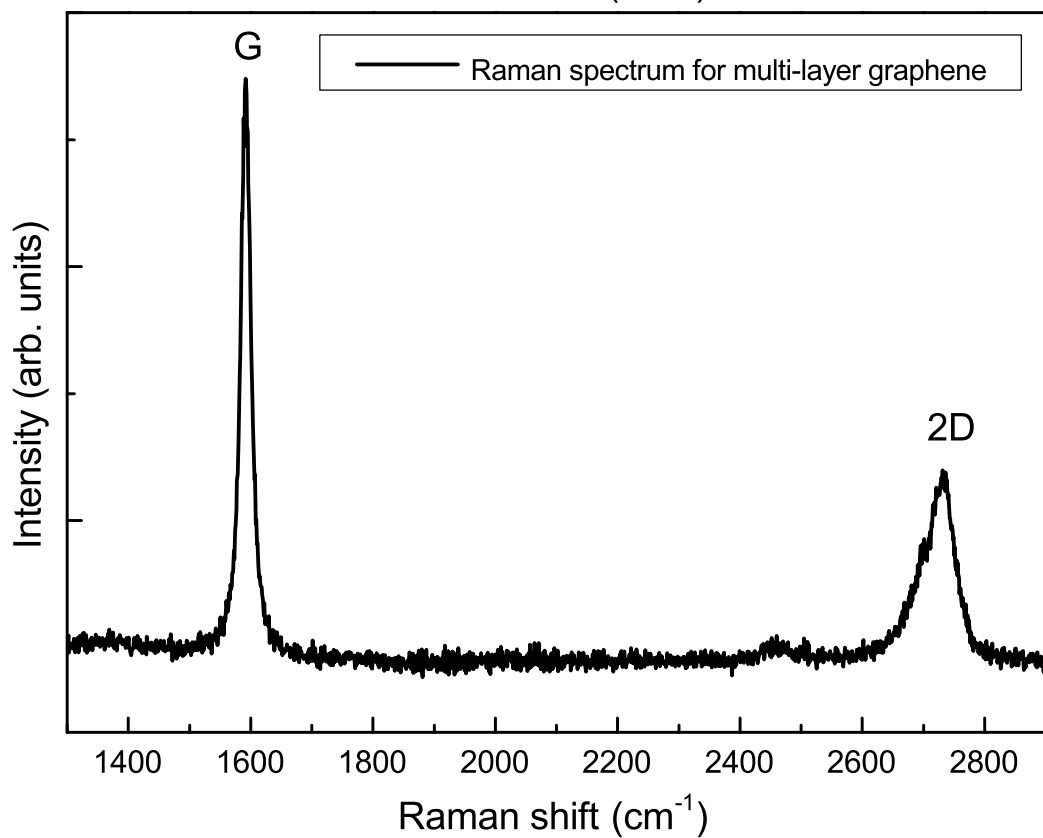
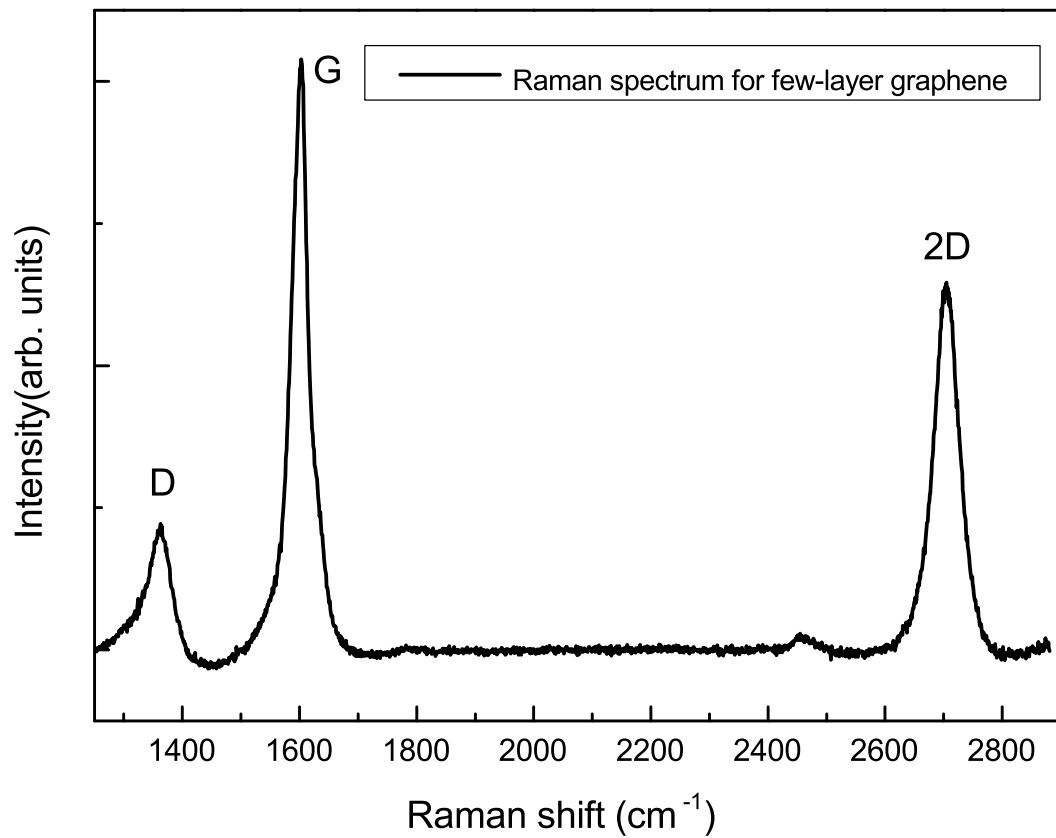


Figure 5.5. Raman spectrum for the few and multi-layer graphene.

5.2. Fabrication of Substrates with Cavities

Samples are prepared with doped silicon wafers ($500\ \mu\text{m}$ in thickness) with $300\ \text{nm}$ silicon oxide on top, in which shallow wells are created with optical lithography techniques and RIE method. After standard cleaning techniques applied on Si/SiO_2 wafers, the wafers are coated with positive type photoresist. Ultra Violet (UV) light is exposed to wafer over the optical lithography mask. The pattern of mask is transferred to photoresist on wafer as changing the chemical structure of photoresist interacting with light. Then the chemically changed photoresist material is removed by a solution named as developer. After that, the structure is exposed by reactive ions and etched. During reactive ion etching the photoresist which is unexposed to light is used as protective layer. The etching is done until creating shallow wells of $300\ \text{nm}$. Moreover, the deposition of $\approx 3\ \text{nm}$ of Ti/Au is realized in order to make graphene more visible after the transfer. After the removal of photoresist, the cavity is formed and the procedure is schematized in Figure 5.6.

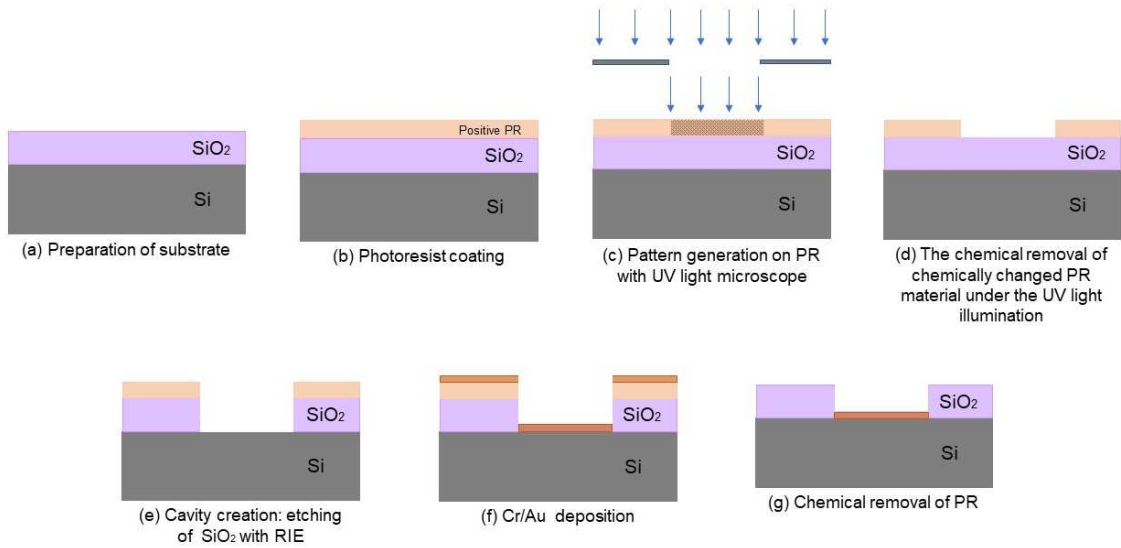


Figure 5.6. Schematic representation of micro cavity fabrication (a) cleaning of substrate on which the cavity structures will be fabricated, (b) spin coating of photoresist material, (c) UV lithography, (d) development of photoresist, (e) anisotropic etching of SiO_2 layer with RIE technique, (f) Cr/Au deposition, (g) chemical removal of photoresist.

After the fabrication of structures with cavities, height profile analyses are done by AFM and stylus profiler. In Figure 5.7, $\approx 300\ \text{nm}$ deep AFM height profile analysis

data is given for a cavity which is $35 \mu m$ in diameter (left) and $\approx 2 \mu m$ deep stylus profiler analysis data is given for a cavity which is $70 \mu m$ in diameter (right).

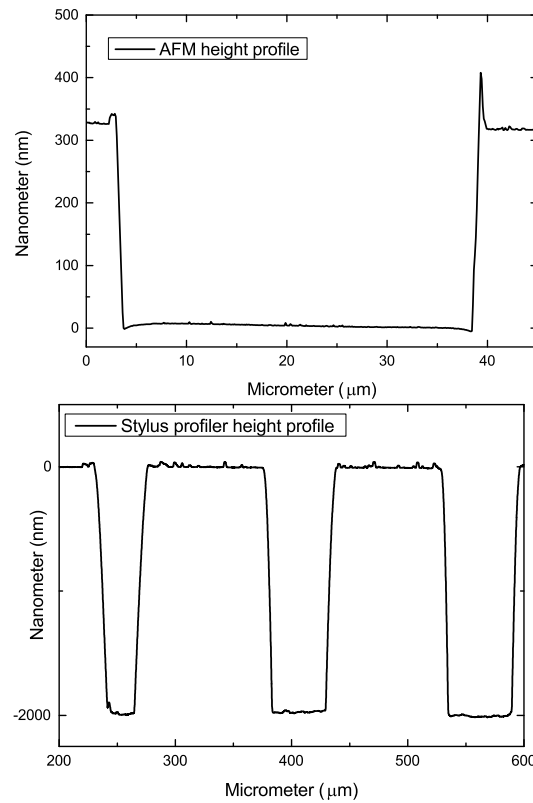


Figure 5.7. AFM height profile (approximately 300 nm) for a cavity with $35 \mu m$ diameter (left). Stylus profiler height profile (approximately $2 \mu m$) for a cavity with $70 \mu m$ diameter (right).

By taking into consideration some research questions, the optical lithography mask is designed for micro fabrication of cavities on SiO_2/Si samples. The optical microscope images of these cavity structures are also presented in the Figure 5.8. The arrays of cavities cover an area of $2 \text{ mm} \times 2 \text{ mm}$. On each sample, different sized cavities are fabricated with cavity diameters ranging from 2 to $100 \mu m$. Circular and hexagonal shapes are selected for cavity formation. Various distances ($10R$, R , $R/2$, $R/10$) between cavities are chosen in the design, where, R is the cavity diameter. The design also includes both air and vacuum gap devices. Mixed diameter arrays are also included to examine the effect of membrane diameter on the device formation.

After the preparation of cavity structures and height profile analyses, the samples are cleaned with standard cleaning procedure, and O_2 plasma treatment is applied in order to increase the adhesion force between graphene and substrate during transfer.

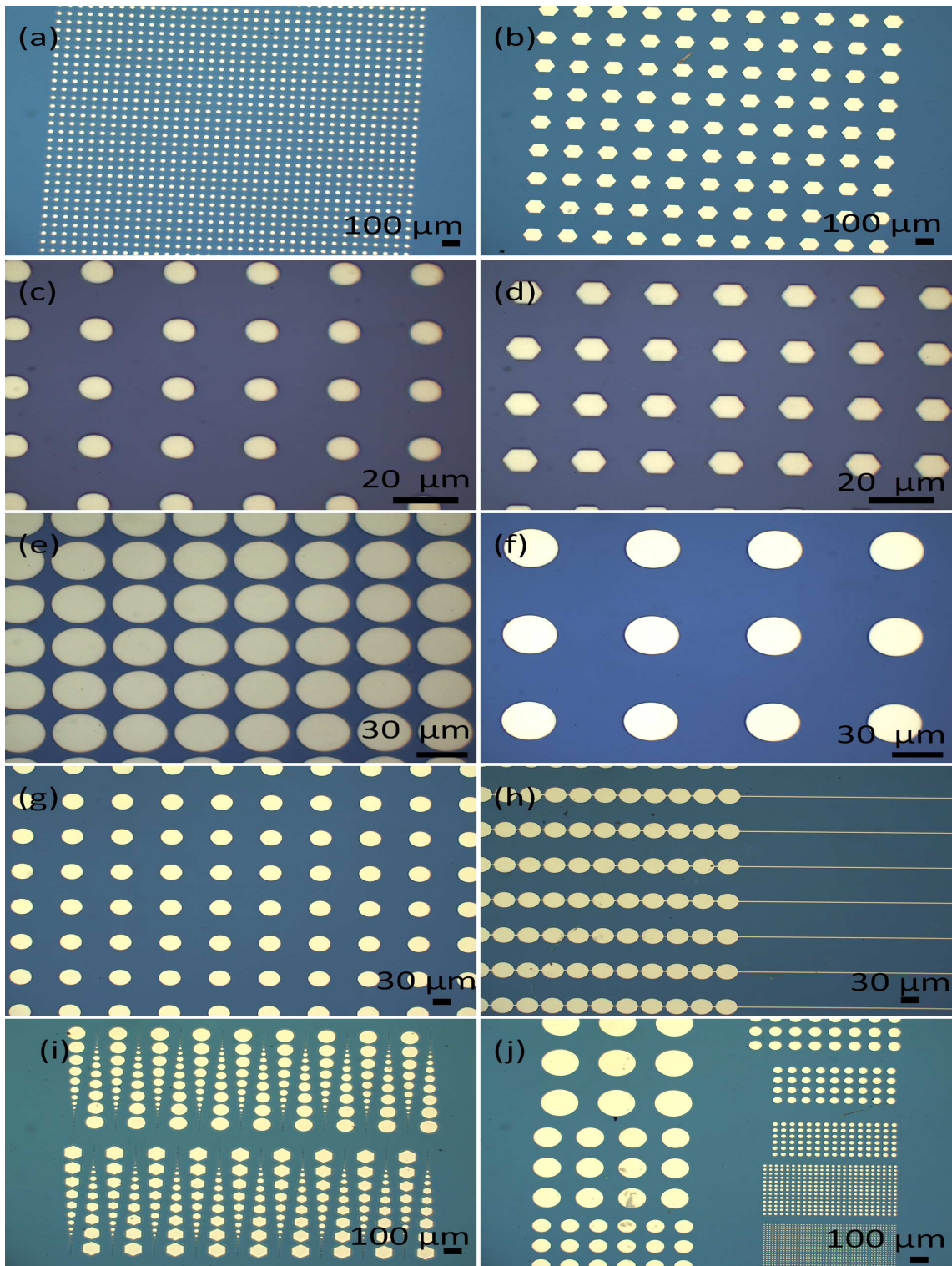


Figure 5.8. Optical microscope images of cavity structures used in the thesis study. (a) $10 \mu m$ cavities, (b) $100 \mu m$ cavities, (c) circular cavities, (d) hexagonal cavities, (e) $R/10$ cavity distance with diameter R , (f) R cavity distance, (g) air gap device cavities, (h) vacuum gap device cavities, (i) and (j) show the cavities with different diameters.

5.3. Support Materials for the transfer of APCVD Grown Graphene on the Substrates with Cavities

The fabrication steps are very critical for the fabrication of membrane structures and quality. Especially, removing support polymer which is used for handling graphene without any contamination on graphene layer is very important for the quality of resulting device. To create micromembranes with a 2D material is a challenging step since atomically thin graphene can be easily damaged or collapsed during the transfer process. That is why a support material is decided to coat on the top side of the graphene/Cu/graphene foil substrate for protection and support. The schematic of the standard transfer technique steps used in this thesis study is shown in Figure 5.9.

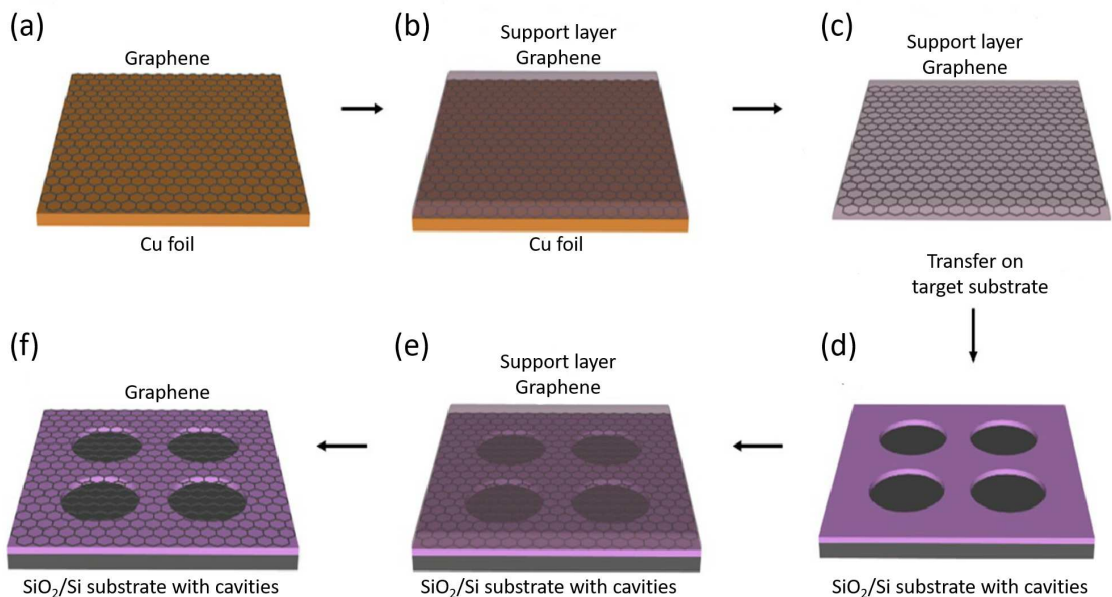


Figure 5.9. Schematized standard transfer technique: (a) graphene on Cu foil, (b) coating a support material on graphene top layer, (c) chemical etching of Cu foil, (d) SiO₂/Si substrate with cavities where the graphene will be transferred on, (e) adhesion of the graphene on the target substrate (f) removal of the support material.

As also shown in Figure 5.9 the transfer of graphene on target cavity structures are done by using support materials. After CVD growth of graphene, the resulting sample is graphene on both faces of copper foil (a). Top of the sample is coated with different supportive layers via drop method or spin coating technique (b), after the support material

is dried and adhere on the top graphene layer, the graphene on bottom is removed by using O_2 plasma technique. Next step is the removal of Cu foil with a 1M ferric chloride $FeCl_3$ in DI water. After the Cu foil is completely etched away, the solution ($FeCl_3$) is transferred to HCl:DI water solution prepared with volume ratio of 1:3 to rinse off any impurity and residue of $FeCl_3$ and then rinsed with DI water. If the thickness of support material is too thin and breakable to carry graphene, the transfer method realized with wet transfer techniques. That means graphene and target substrate interaction is realized when the graphene is floating on DI water. The support layer/graphene structures are not scooped, but the solution where the graphene floating is changed with a help of syringe. After the transfer, the sample is waited at a hot ($90\text{ }^\circ\text{C}$) plate for 45 seconds to create adhesion between graphene and SiO_2 surface with van der Waals forces.

After the graphene transfer using a supportive layer, the removal of support material is realized (f). As a support material photoresist, PMMA, PDMS, thermal release tape and their combinations with PMMA are studied. For each support material, the removal method is also different. The removal methods according to support material is presented in Figure 5.10.

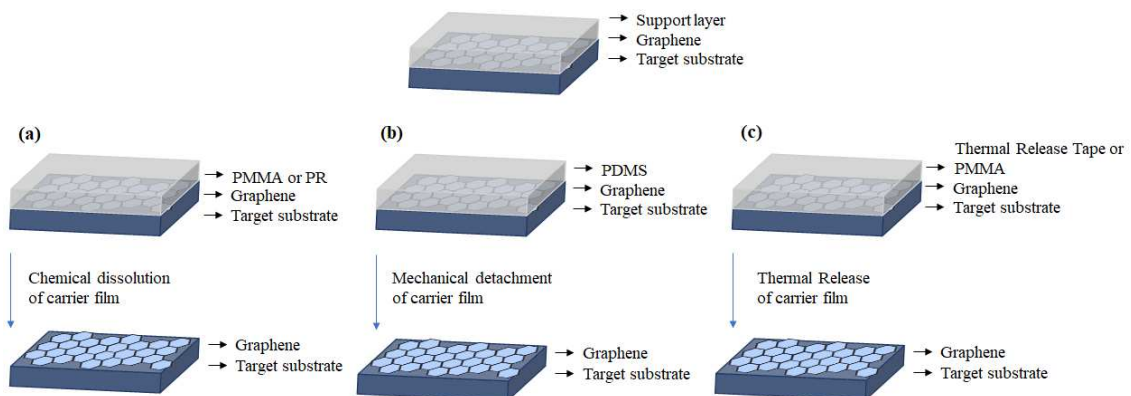


Figure 5.10. Schematic which illustrates detachments of carrier films during standard transfer method.

While the removal of photoresist is realized by using chemical etching, the removal of PMMA support is studied with using chemical etching and thermal treatment. Besides, the PDMS layer is removed with mechanical detachment. Transfer approaches on substrate with micro scale cavities by using different support layers is presented in the following sections.

5.3.1. Photoresist

The transfer of graphene on cavity structures is realized with S1813 type photoresist as a transfer support material. After the Cu foil is etched away, the transfer is realized with dry technique. The samples which have cavity depths of 300 nm to 2 μm are studied. After the transfer, the removal of photoresist material is done by using acetone. The samples are analysed with AFM by measuring the height profiles of randomly selected cavities. These measurement show that the membranes are collapsed to the bottom layer. The SEM image of a sample of this method which has 10 μm cavity diameter and 300 nm cavity depth is presented in Figure 5.11.

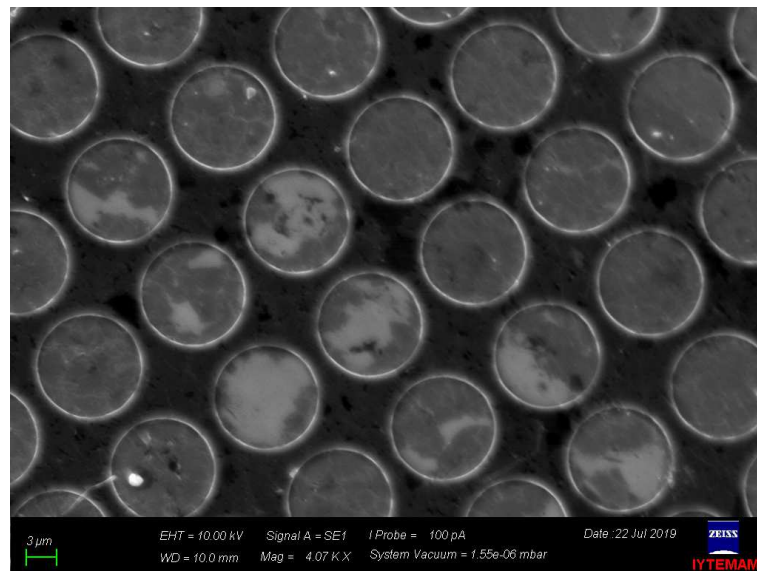


Figure 5.11. SEM image after graphene transfer on 10 μm cavity structure by using S1813 type photoresist material.

5.3.2. PMMA

As a second transfer approach, graphene transfer is realized by using PMMA material. After CVD growth, graphene on Cu foil is covered with PMMA material with spin coating technique (4000 rpm for 45 seconds). After the coating, the sample is waited 12 hour at room temperature in order to solidify PMMA. While PMMA on graphene is floating on DI water, the graphene and PMMA is scooped out with a sample which has cavity

structures on it. After the transfer, the SiO₂/Si/grp/PMMA heterostructure is left to dry to create adhesion of graphene to the substrate. While applying this transfer approach, different PMMA removal techniques are tried. These are the chemical etching in acetone and thermal removal methods.

The prepared samples are examined by using optical microscope and AFM tools. The optical microscope image of PMMA transferred graphene is given in the Figure 5.12. As seen in Figure 5.12, all the transfer approaches are realized to the half side of the cavity structures. The reason of this is to compare AFM height profile analysis of cavities before and after the transfer. AFM height profiles taken randomly from various cavities do not show suspended structures. Figure 5.13 (a) and (b) show the cavity before and after the transfer, respectively.

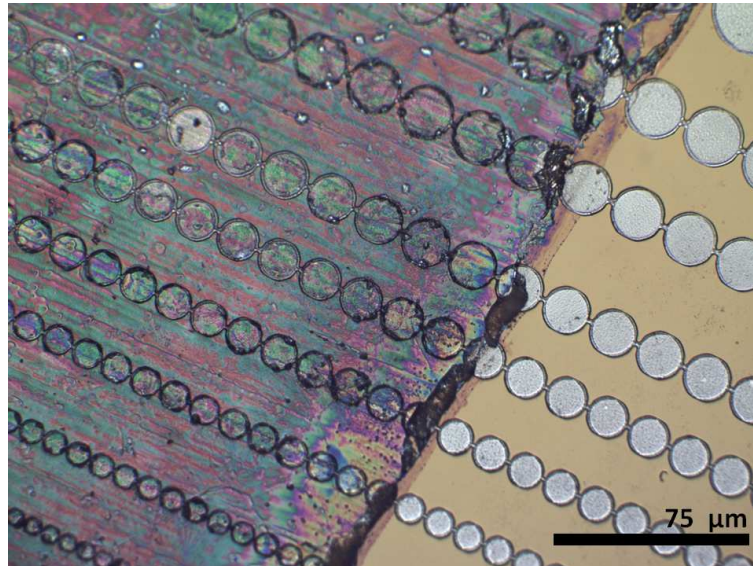


Figure 5.12. Optical microscope image of graphene transfer via PMMA support material on cavity structures of changing diameters.

5.3.3. Photoresist & PMMA

For this approach, combination of S1813 photoresist and PMMA is used. If the support material is only a PMMA layer, wet transfer technique needs to be used. In this approach, photoresist is used for handling the thin PMMA layer and transferring graphene with dry technique. The AFM height profiles are collected from randomly chosen cavity

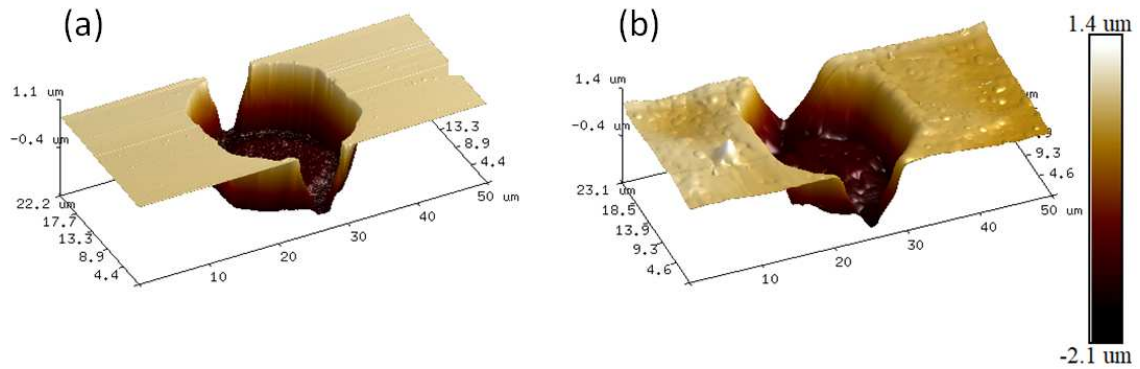


Figure 5.13. 3D AFM height profile for a substrate before (a) and after (b) transfer.

structures that have various diameters. These analyses show the same height profiles before and after the transfer.

Figure 5.14 presents SEM images of a broken membrane structure after the removal of photoresist on a $5\ \mu\text{m}$ cavity structure. Here, Figure 5.14 (a) presents the broken membrane with a magnification of 40 kx, Figure 5.14 (b) presents the same cavity structure with 100 kx magnification.

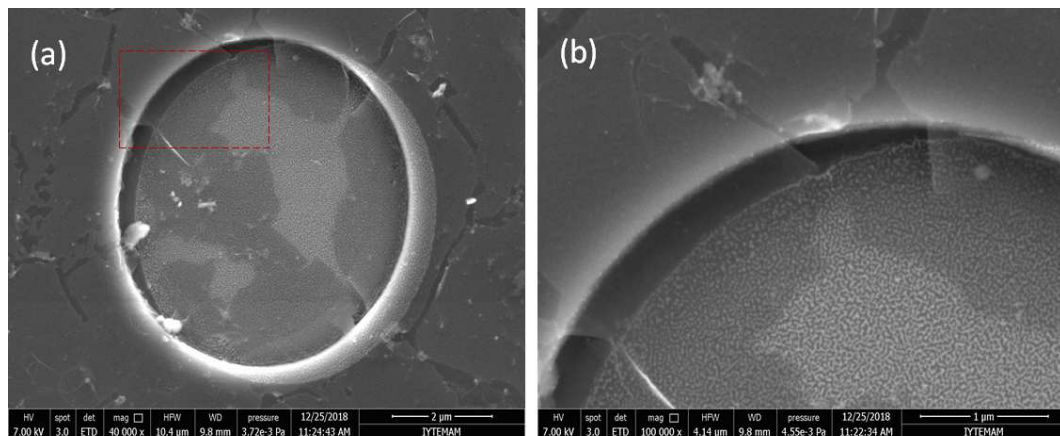


Figure 5.14. SEM image of mono-layer graphene transfer by using PDMS & PMMA heterostructure as a support material. (a) cavity structure with graphene layer after the transfer, (b) close up view of the same cavity indicated by red dashed square.

5.3.4. PDMS

As being one of the graphene transfer approach, PDMS is used as graphene support layer. The removal of PDMS is done with mechanical detachment technique which offers easy removal process without any chemical etching process. After the CVD growth of graphene on Cu foil, the liquid PDMS material is dropped. After the solidification of PDMS at room temperature, Cu foil is etched with standard chemical etching procedure. Then dry transfer is realized on the substrates with cavities. The samples which have mixed diameter arrays are used. After the heat treatment is applied to create adhesion between graphene and SiO₂, the removal of PDMS is realized with mechanical detachment.

The SEM image presenting the sample fabricated with this transfer method is given in Figure 5.15. The cavities on the image are 20 μm in diameter and 300 nm in depth. The graphene over the edges of cavities looks damaged during the transfer.

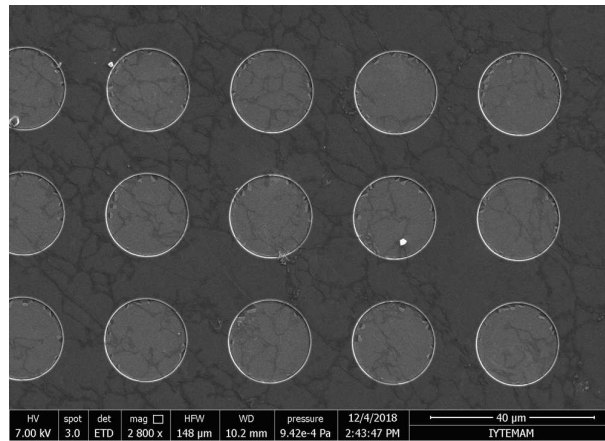


Figure 5.15. SEM image of structures with cavities after the transfer via thermal release tape.

5.3.5. PDMS & PMMA

For the transfer approach where the mono-layer graphene supported with PDMS & PMMA, graphene on Cu foil is firstly covered with PMMA and then PDMS material is dropped on the structure. After the etching of Cu foil, the dry transfer of graphene is realized on the cavity structures. PDMS stamp is removed with mechanical detachment technique and PMMA removal is done with thermal treatment. Thermal removal of

PMMA is realized in a furnace with vacuum at 200 °C for 2 hours. To increase optical contrast during SEM analysis of membrane structures, 2 nm Au layer is deposited inside the cavity structures. During deposition of gold with metal evaporation technique a 500 nm shift is observed because of misalignment of the sample. The shift can be clearly seen in the SEM images.

The SEM image of graphene membranes is given in Figure 5.16. While Figure 5.16 (a) presents a homogeneous and suspended mono-layer graphene membrane structure over a 2 μm cavity structure with 300 nm depth, Figure 5.16 (b) presents a broken membrane structure with the same cavity properties. Moreover, Figure 5.17 is given to show the differences between a ruptured membrane (Figure 5.17 (a)) and a broken membrane (Figure 5.17 (b)) structures. Additionally, in Figure 5.18, a half suspended membrane structure over the 2 μm cavity is presented.

The AFM height profile and image of this graphene membrane over the 2 μm cavity structure after PMMA removal with thermal treatment is given in Figure 5.19. The AFM measurement presents an ~ 150 nm membrane deformation profile over a 300 nm cavity. The AFM height profiles also collected from the graphene membranes having larger cavity diameters. The AFM height profile and 3D image of an ~ 4 μm graphene membrane over 300 nm depth cavity structure is given in Figure 5.20, presenting cavity structure before and after the transfer. The AFM height profile image and 3D image of a graphene membrane over 5 μm cavity structure is presented in Figure 5.21 with an ~ 125 nm suspended membrane profile.

5.3.6. Thermal Release Tape

In this approach, as a support material during graphene transfer, thermal release tape is used. After CVD growth of mono-layer graphene on Cu foil, thermal release tape is attached on the graphene with applying a pressure. Then, Cu foil is removed with chemical etching procedure and graphene with thermal release tape is transferred on the structure with cavities. To create adhesion between graphene and target cavity structure and to remove thermal release tape, the sample is waited on a hot plate at 100 °C. A lot of transfer approaches are ended up with failed adhesion of graphene layers from thermal release tape to the sample of interest. The ones that adhere on the SiO₂/Si samples showed collapsed behaviour at the AFM height profile analysis. The optical image showing an example of thermal release tape transfer is given in Figure 5.22.

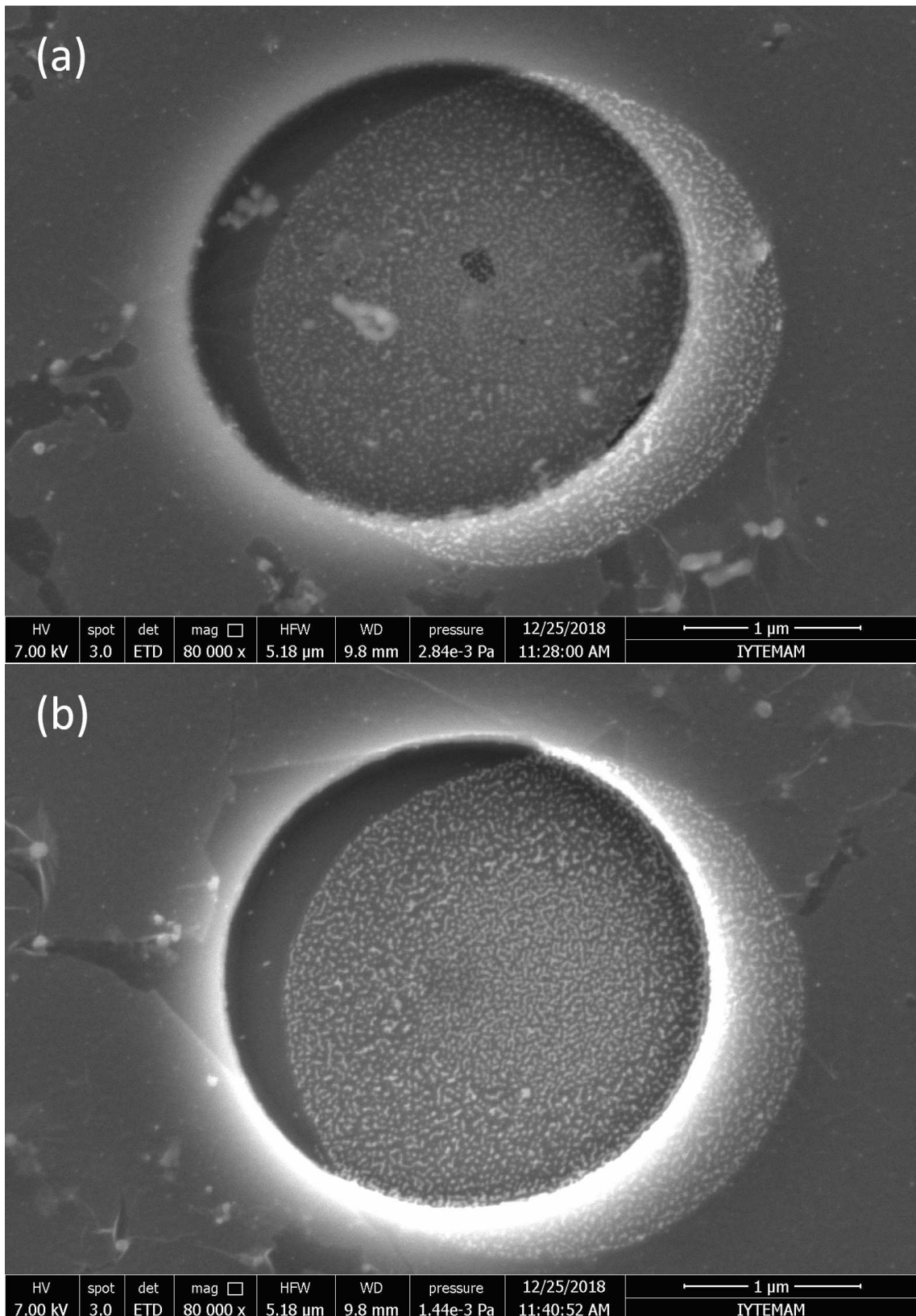


Figure 5.16. SEM image of suspended (a) and broken (b) membrane structures, transferred via PDMS& PMMA support layer.

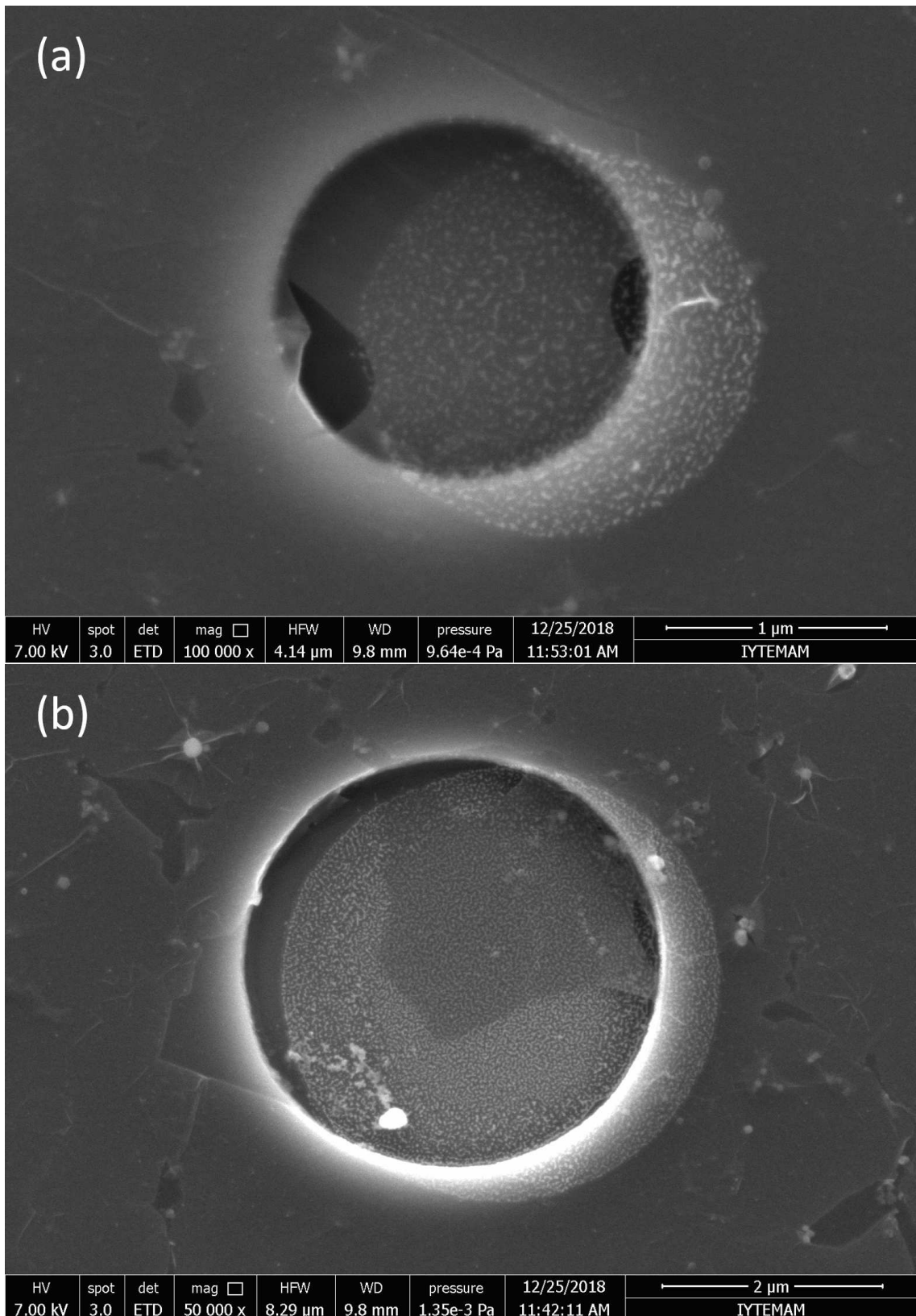


Figure 5.17. SEM image of (a) a ruptured and (b) broken mono-layer graphene membrane structures transferred via PDMS & PMMA support layer.

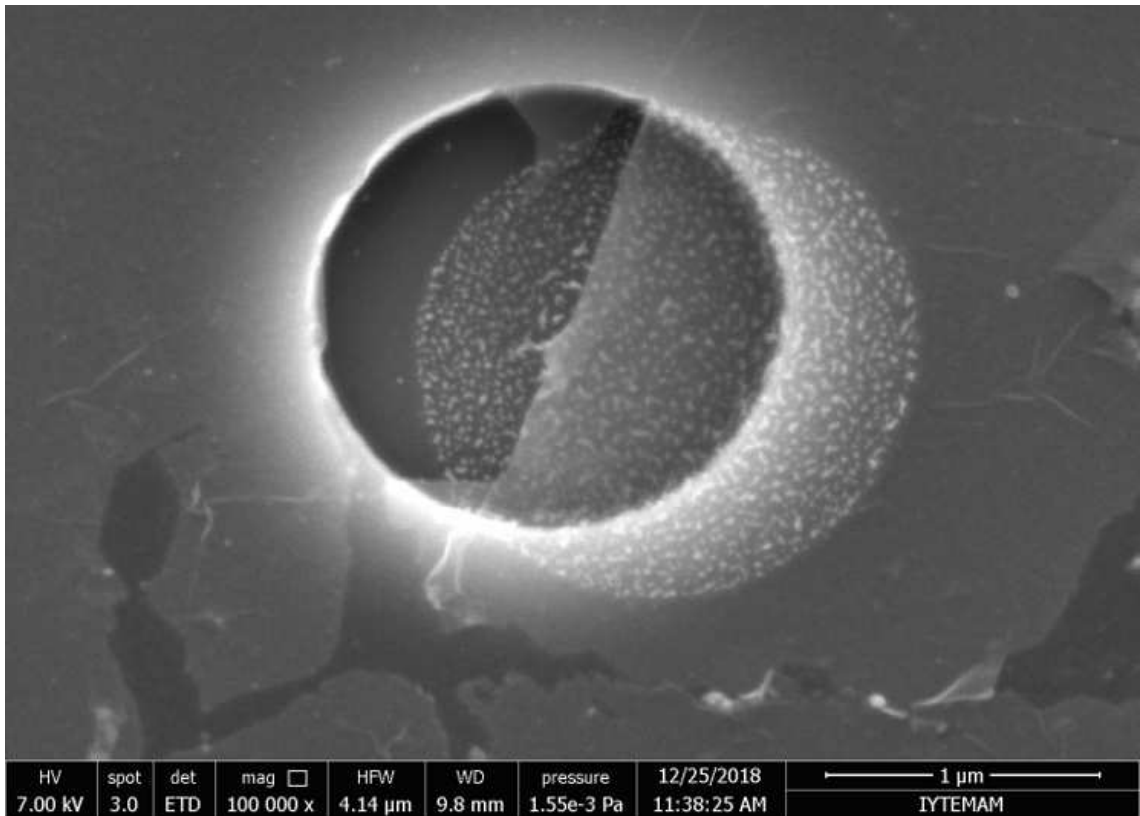


Figure 5.18. SEM image of a mono-layer graphene half membrane structure transferred with PDMS & PMMA support layer.

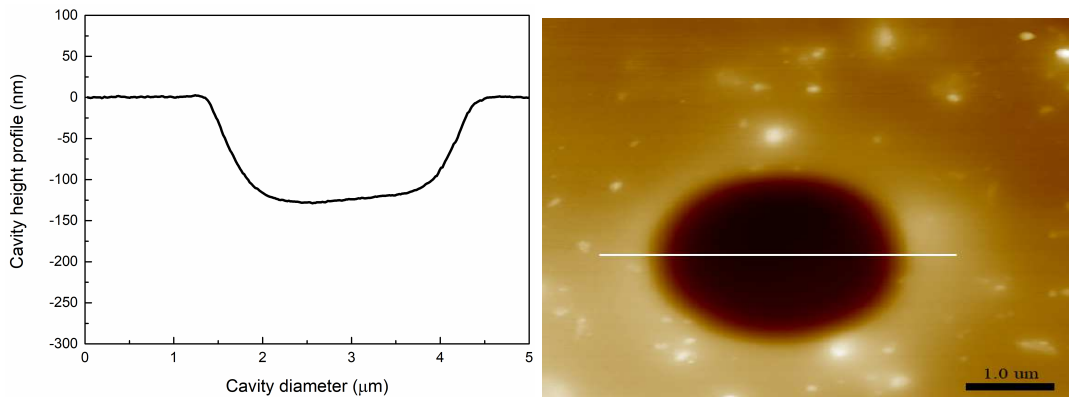


Figure 5.19. AFM height profile (top) and 3D image (bottom) of a graphene membrane over a 300 nm deep cavity with $\sim 2 \mu\text{m}$ diameter. White line on the right image shows the path where the height profile is taken.

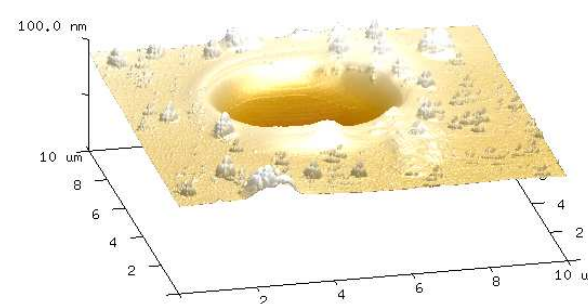
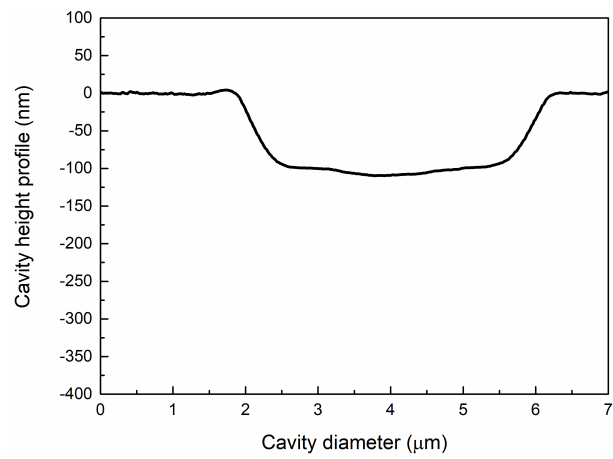
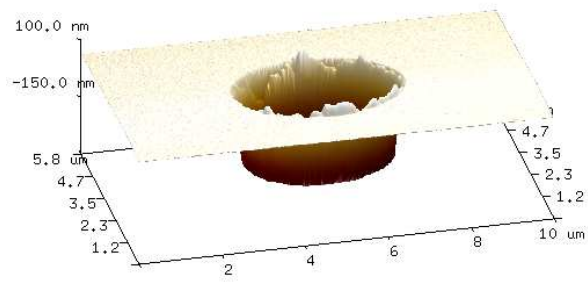
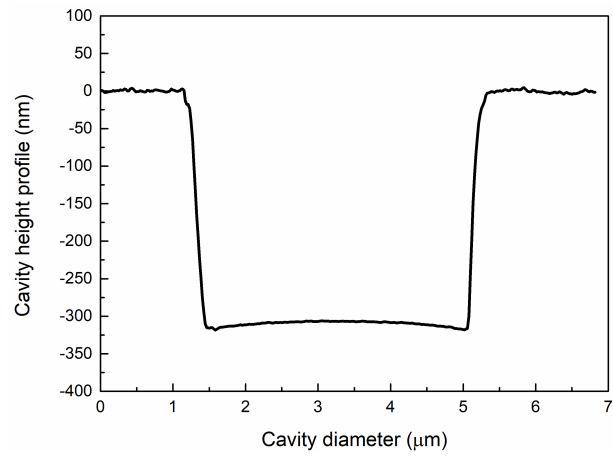


Figure 5.20. AFM height profiles (first and second) and 3D images (third and fourth) of $\sim 4 \mu\text{m}$ cavity structures before (left) and after (right) graphene transfer via PDMS & PMMA support layer.

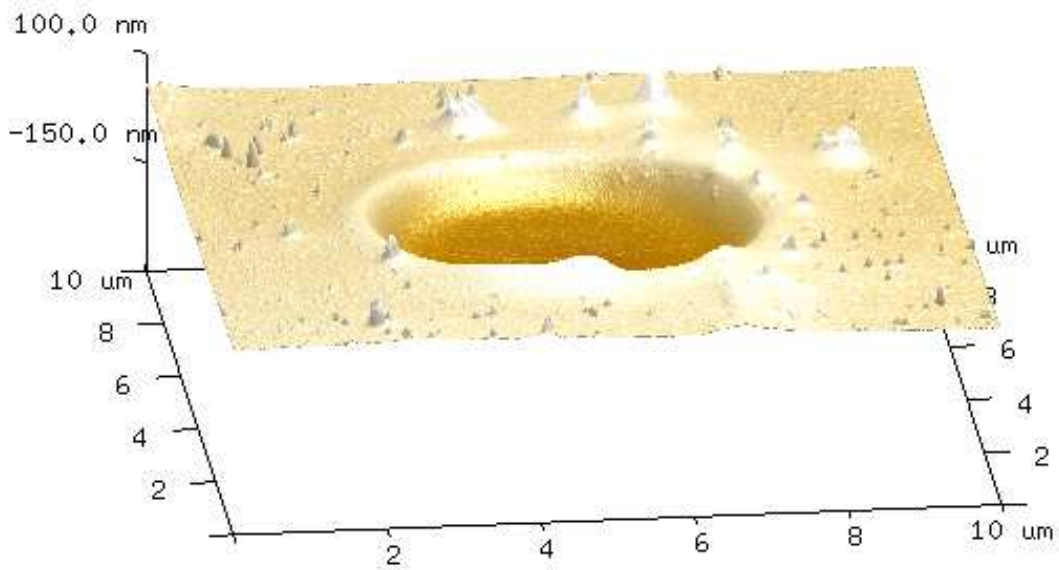
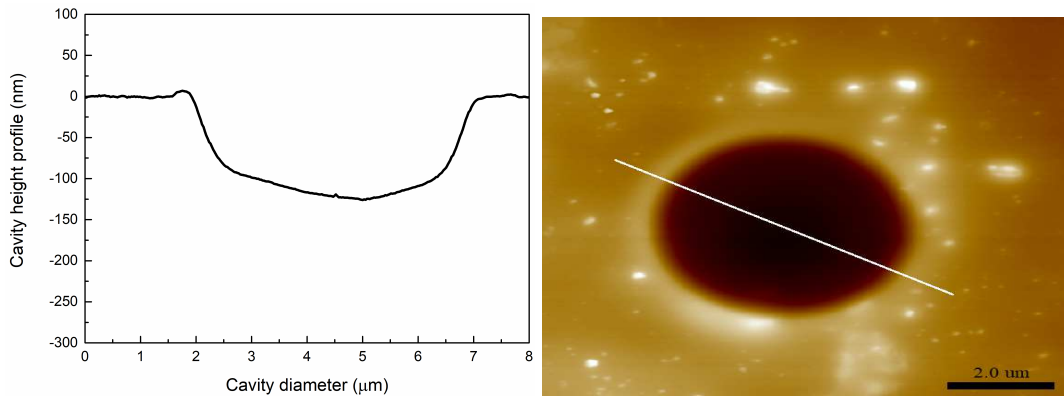


Figure 5.21. AFM height profile and image of a graphene membrane over a 300 nm deep cavity with $\sim 5 \mu\text{m}$ diameter. White line on the right image shows the path where the height profile is taken.

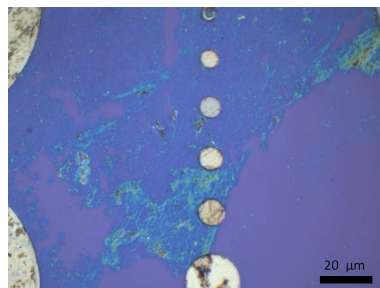


Figure 5.22. Optical image of a mono-layer graphene transferred on cavity structures via thermal release tape as support material.

5.3.7. Thermal Release Tape & PMMA

As a last transfer approach, after CVD growth of graphene on Cu foils, the graphene on the top side of the Cu foil is coated with PMMA. After PMMA is dried at room temperature, thermal release tape is attached on PMMA layer. Then, Cu foil is removed with chemical etching and graphene is transferred on the half side of pre-cleaned Si/SiO₂ samples with cavities. O₂ plasma treatment is also applied on the cavity structures just before the transfer is realized. After the transfer, the adhesion of graphene on the sample and removal of thermal release tape are done with heat treatment. Figure 5.23 shows the optical microscope image of a PMMA/graphene structure after the transfer with thermal release tape on cavity structures with different diameters.

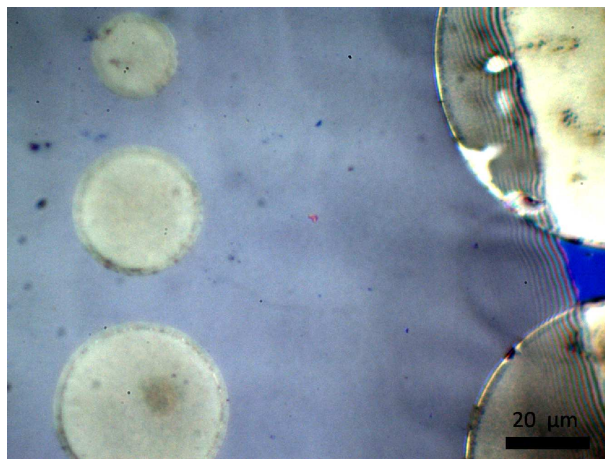


Figure 5.23. Optical microscope image of graphene transfer via thermal release tape & PMMA as support layer. Transfer is applied on samples which have cavity structures of changing diameters.

5.3.8. Discussion

All the transfer approaches with different support layers have their own advantages and disadvantages. When we used photoresist as a support material, we observed residues on the graphene layer after the transfer. But when the etching and cleaning steps were repeated several times, the amount of residues was decreased. Meanwhile, wet chemical etching of photoresist in acetone can be a reason of membrane collapse.

The handling of graphene layer with PMMA is challenging because of the fragile nature of PMMA film. For this reason, the transfer via PMMA support layer was realized with the fishing method in DI water (wet transfer). But, during the wet transfer the liquid could be trapped inside the cavities. Moreover, the removal of PMMA with chemical etching ends up with PMMA residues on the graphene layer and the thermal annealing is needed.

For the transfer approach with PDMS, there are also some constraints and advantages. Mechanical detachment of PDMS layer is dry and clean technique which does not need any chemical steps. However, the detachment can cause membrane tears during mechanical pulling.

Most of the time when we used the thermal release tape as a support layer, we observed no or partial adhesion of graphene layer to the substrate. To understand the reason of this, mono-layer graphene on Cu foils and multi-layer graphene on Ni foils were used. The chemical etching of metal foils were repeated several times (with different heat treatment procedures) to make sure that the metal residues (which can affect adhesion of graphene) are completely removed, but, the adhesion of graphene on target substrate was not achieved. Complete removal of the metal foil was confirmed by the Raman analysis. The low yield of the transfer makes this technique less preferable compared to the other methods. Summary of all the transfer approaches used in this study is given in table 5.2.

Table 5.2. Summary of transfer approaches used in this study

Section number	Graphene		Cavity Structure			Transfer Approach		
	Graphene synthesis	Number of layers	Cavity diameter (R)	Cavity height	Distance between cavities	Support material	Interaction	Removal of support material
5.3.1	CVD setup/ Graphene S.	Mono/few layer Multi layer	$2 - 100 \mu m$	$300 nm$ $- 2 \mu m$	$R/10$ $10R$	S1813 PR	Dry	Chemical etching
5.3.2	CVD Setup/ Graphenia	Mono/few layer	$2 - 100 \mu m$	$300 nm$ $- 2 \mu m$	$R/10$ $10R$	PMMA	Wet	Chemical etching & Thermal treatment
5.3.3	CVD Setup	Mono/few layer	$2 - 100 \mu m$	$300 nm$	$10R$	PR & PMMA	Dry	Chemical etching
5.3.4	CVD Setup	Mono/few layer	$2 - 100 \mu m$	$300 nm$	$R/2$ $10R$	PDMS	Dry	Mechanical detachment
5.3.5	CVD Setup	Mono/few layer	$2 - 100 \mu m$	$300 nm$	$10R$	PDMS & PMMA	Dry	Mechanical detachment & Thermal treatment
5.3.6	CVD Setup	Mono/few layer	$2 - 100 \mu m$	$300 nm$	R $10R$	T. release tape	Dry	Thermal treatment
5.3.7	CVD Setup	Mono/few layer	$2 - 100 \mu m$	$300 nm$	R $10R$	Thermal release tape & PMMA	Dry	Thermal treatment

CHAPTER 6

CONCLUSION AND FUTURE WORK

In this thesis, fabrication and characterization of graphene micro membrane structures are studied. Fabricating membranes with a 2D material and the characterization of these membranes is an experimental procedure including the steps of synthesis of graphene, fabrication of cavity structures and transfer of synthesized graphene on cavity structures.

Uniform, scalable, and transferable large area mono and few layer graphene on Cu foils are synthesized with APCVD technique. Raman spectroscopy characterization is performed after the transfer of graphene on flat substrates. The substrates with 300 nm cavities are fabricated with optical lithography and RIE techniques. Circular and hexagonal micro-cavities have diameters ranging between 2-100 μm and depths of 300 nm and 2 μm . Before the transfer, structures with cavities are cleaned with standard cleaning procedures and O₂ plasma treatment. CVD graphene on growth substrate is coated with support material and the transfer is realized after chemical etching of Cu foil.

Photoresist, PMMA, PDMS, thermal release tape and their combinations with PMMA are used as support materials. The transfer is realized on the half side of cavity arrays in order to compare the cavity depths before and after the transfer. After the transfer, the adhesion of graphene to SiO₂ is achieved via heat treatment. The removal of support material is chosen according to the properties of support material. Optical microscope, SEM and AFM tools are used for characterization of the fabricated samples.

In the study, advantages and disadvantages of the support materials used are investigated in terms of handling, interaction with cavity structure, removal, and residue removal aspects. All the outcomes can be summarized as follows: Using the PMMA layer in between graphene and the other support layer is advantageous. Because, the transfer by using only PMMA needs the wet transfer steps where the liquid could be trapped inside the cavities. Using an additional layer changes the transfer into the dry transfer. Choosing PDMS & PMMA as a support layer is advantageous because of the dry removal and ease of apply. The thermal removal of the PMMA can also be done by chemical free step to protect membrane structures even though PMMA removal ends up with residues.

AFM analyses of mono-layer CVD graphene transferred via PDMS & PMMA layer show suspended behaviour having the membrane deformation profiles ranging from

$\sim 100 \text{ nm}$ to $\sim 150 \text{ nm}$ on a 300 nm depth cavity structures with $2\text{-}5 \mu\text{m}$ cavity diameters. On the same sample, the graphene membranes are observed as collapsed or broken for the cavities larger than $5 \mu\text{m}$.

SEM images of suspended membranes comply with the AFM results. Additionally, SEM analysis give further information about tears, inhomogeneities, and broken parts of the graphene membrane structures.

Planned future studies for the fabrication and characterization of graphene micro-membranes can be stated as follows: The transfer will be done by using multi-layer graphene samples synthesized on Ni foils. For this purpose, the adhesion of bulk ($\sim 500 \text{ nm}$) multi-layer graphene to the target substrate will be investigated in detail. To reduce the number of layers plasma treatment will be studied. The direct transfer approach will be studied to fabricate micro-membranes in larger dimensions. To reduce the residues remaining from PMMA, chemical etching and thermal treatment steps will be optimized. Finally, the stiffness of the graphene micro membranes will be obtained by using AFM force-distance measurements.

REFERENCES

- AbdelGhany, M., F. Mahvash, M. Mukhopadhyay, A. Favron, R. Martel, M. Siaj, and T. Szkopek (2016). Suspended graphene variable capacitor. *2D Materials*.
- Alemán, B., W. Regan, S. Aloni, V. Altoe, N. Alem, C. Girit, B. Geng, L. Maserati, M. Crommie, F. Wang, and A. Zettl (2010). Transfer-free batch fabrication of large- Area suspended graphene membranes. *ACS Nano*.
- Arjmandi-Tash, H., A. Allain, Z. Han, and V. Bouchiat (2017). Large scale integration of CVD-graphene based NEMS with narrow distribution of resonance parameters. *2D Materials*.
- Atalaya, J., A. Isacson, and J. M. Kinaret (2008). Continuum elastic modeling of graphene resonators. *Nano Letters* 8(12), 4196–4200. PMID: 18956921.
- Batzill, M. (2012). The surface science of graphene: Metal interfaces, CVD synthesis, nanoribbons, chemical modifications, and defects.
- Beams, R., L. G. Cançado, and L. Novotny (2015, jan). Raman characterization of defects and dopants in graphene. *Journal of Physics: Condensed Matter* 27(8), 083002.
- Berger, C., R. Phillips, A. Centeno, A. Zurutuza, and A. Vijayaraghavan (2017). Capacitive pressure sensing with suspended graphene–polymer heterostructure membranes. *Nanoscale* 9(44), 17439–17449.
- Blake, P., E. W. Hill, A. H. Castro Neto, K. S. Novoselov, D. Jiang, R. Yang, T. J. Booth, and A. K. Geim (2007). Making graphene visible. *Applied Physics Letters* 91(6).
- Bolotin, K. I., K. J. Sikes, Z. Jiang, M. Klima, G. Fudenberg, J. Hone, P. Kim, and H. L. Stormer (2008). Ultrahigh electron mobility in suspended graphene. *Solid State Communications*.
- Bunch, J. S., A. M. Van Der Zande, S. S. Verbridge, I. W. Frank, D. M. Tanenbaum, J. M. Parpia, H. G. Craighead, and P. L. McEuen (2007). Electromechanical resonators from graphene sheets. *Science*.

- Bunch, J. S., S. S. Verbridge, J. S. Alden, A. M. Van Der Zande, J. M. Parpia, H. G. Craighead, and P. L. McEuen (2008). Impermeable atomic membranes from graphene sheets. *Nano Letters*.
- Caldwell, J. D., T. J. Anderson, J. C. Culbertson, G. G. Jernigan, K. D. Hobart, F. J. Kub, M. J. Tadjer, J. L. Tedesco, J. K. Hite, M. A. Mastro, R. L. Myers-Ward, C. R. Eddy, P. M. Campbell, and D. K. Gaskill (2010). Technique for the dry transfer of epitaxial graphene onto arbitrary substrates. *ACS Nano* 4(2), 1108–1114.
- Cantarero, A. (2015, 12). Raman scattering applied to materials science. *Procedia Materials Science* 9.
- Castro Neto, A. H., F. Guinea, N. M. Peres, K. S. Novoselov, and A. K. Geim (2009). The electronic properties of graphene. *Reviews of Modern Physics* 81(1), 109–162.
- Chong, P.-F., C.-H. Cheng, and X. Shi (2014). Capacitive micromachined ultrasonic transducer (CMUT) array with single-layer graphene membrane. *Micro & Nano Letters* 9(12), 884–886.
- Cooper, D. R., B. D. Anjou, N. Ghattamaneni, B. Harack, M. Hilke, N. Majlis, M. Massicotte, L. Vandsburger, E. Whiteway, and V. Yu (2011). Experimental review of graphene.
- Falkovsky, L. A. (2007, Aug). Phonon dispersion in graphene. *Soviet Journal of Experimental and Theoretical Physics* 105(2), 397–403.
- Ferrari, A. C. and D. M. Basko (2013). Raman spectroscopy as a versatile tool for studying the properties of graphene. *Nature nanotechnology*.
- Frank, I. W., D. M. Tanenbaum, A. M. van der Zande, and P. L. McEuen (2007). Mechanical properties of suspended graphene sheets. *Journal of Vacuum Science & Technology B: Microelectronics and Nanometer Structures* 25(6), 2558.
- Gong, S. C. and C. Lee (2001). Analytical solutions of sensitivity for pressure microsensors. *IEEE Sensors Journal*.
- Graph, Z. H. (2013). Macroscopic CVD Graphene for Nanoelectronics: from growth to

- proximity-induced 2D superconductivity, Ph.D. thesis, University of Grenoble .
- Hallam, T., C. F. Moldovan, K. Gajewski, A. M. Ionescu, and G. S. Duesberg (2015). Large area suspended graphene for nano-mechanical devices. *Physica Status Solidi (B) Basic Research* 252(11), 2429–2432.
- Hiura, H., H. Miyazaki, and K. Tsukagoshi (2010). Determination of the number of graphene layers: Discrete distribution of the secondary electron intensity stemming from individual graphene layers. *Applied Physics Express*.
- Hwangbo, Y., C.-K. Lee, S.-M. Kim, J.-H. Kim, K.-S. Kim, B. Jang, H.-J. Lee, S.-K. Lee, S. S. Kim, J.-H. Ahn, and S.-M. Lee (2014, 03). Fracture characteristics of monolayer cvd-graphene. *Scientific Reports* 4, 4439.
- Khuri-Yakub, B. T. and Ö. Oralkan (2011). Capacitive micromachined ultrasonic transducers for medical imaging and therapy. *Journal of Micromechanics and Microengineering*.
- Kim, W. (2015). Fabrication and characterization of graphene-based electronic devices.
- Kobayashi, T., M. Bando, N. Kimura, K. Shimizu, K. Kadono, N. Umezumi, K. Miyahara, S. Hayazaki, S. Nagai, Y. Mizuguchi, Y. Murakami, and D. Hobara (2013). Production of a 100-m-long high-quality graphene transparent conductive film by roll-to-roll chemical vapor deposition and transfer process. *Applied Physics Letters*.
- Kumar, A. and C. Huei (2013). Synthesis and Biomedical Applications of Graphene: Present and Future Trends. In *Advances in Graphene Science*.
- Ledwosinska, E., P. Gaskell, A. Guermoune, M. Siaj, and T. Szkopek (2012). Organic-free suspension of large-area graphene. *Applied Physics Letters*.
- Lee, C., X. Wei, J. W. Kysar, and J. Hone (2008). Measurement of the elastic properties and intrinsic strength of monolayer graphene. *Science*.
- Lee, C. K., Y. Hwangbo, S. M. Kim, S. K. Lee, S. M. Lee, S. S. Kim, K. S. Kim, H. J. Lee, B. I. Choi, C. K. Song, J. H. Ahn, and J. H. Kim (2014). Monatomic chemical-vapor-deposited graphene membranes bridge a half-millimeter-scale gap. *ACS Nano*.

- Lee, G.-h. (2015). (Science) High-strength chemical vapor deposited graphene and grain boundaries. *280780143*(August).
- Lee, J., X. Zheng, R. C. Roberts, and P. X. Feng (2015). Scanning electron microscopy characterization of structural features in suspended and non-suspended graphene by customized CVD growth. *Diamond and Related Materials* 54(1), 64–73.
- Li, X., W. Cai, J. An, S. Kim, J. Nah, D. Yang, R. Piner, A. Velamakanni, I. Jung, E. Tutuc, S. K. Banerjee, L. Colombo, and R. S. Ruoff (2009). Large-area synthesis of high-quality and uniform graphene films on copper foils. *Science*.
- Li, X., W. Cai, L. Colombo, and R. S. Ruoff (2009). Evolution of graphene growth on Ni and Cu by carbon isotope labeling. *Nano letters*.
- Li, X., C. W. Magnuson, A. Venugopal, R. M. Tromp, J. B. Hannon, E. M. Vogel, L. Colombo, and R. S. Ruoff (2011). Large-area graphene single crystals grown by low-pressure chemical vapor deposition of methane on copper. *Journal of the American Chemical Society*.
- Liechti, K. M., R. Huang, J. W. Suk, D. Akinwande, L. Tao, R. S. Ruoff, and S. R. Na (2015). Selective Mechanical Transfer of Graphene from Seed Copper Foil Using Rate Effects. *ACS Nano* 9(2), 1325–1335.
- Liu, L. L., O. M. Mukdadi, C. F. Herrmann, R. A. Saravanan, J. R. Hertzberg, S. M. George, and V. M. Bright (2004). A Novel Method for Fabricating Capacitive Micromachined Ultrasonic Transducers with Ultra- Thin Membranes. *IEEE Transactions on Ultrasonics Ferroelectrics and Frequency Control* 1, 497–500.
- Mattevi, C., H. Kim, and M. Chhowalla (2011). A review of chemical vapour deposition of graphene on copper. *Journal of Materials Chemistry*.
- Mermin, N. D. (1968, Dec). Crystalline order in two dimensions. *Phys. Rev.* 176, 250–254.
- Meyer, J. C., A. K. Geim, M. I. Katsnelson, K. S. Novoselov, T. J. Booth, and S. Roth (2007). The structure of suspended graphene sheets. *Nature*.
- Na, S. R., J. W. Suk, L. Tao, D. Akinwande, R. S. Ruoff, R. Huang, and K. M. Liechti

- (2015). Selective mechanical transfer of graphene from seed copper foil using rate effects. *ACS Nano*.
- Nair, R. R., P. Blake, A. N. Grigorenko, K. S. Novoselov, T. J. Booth, T. Stauber, N. M. R. Peres, and A. K. Geim (2008). Fine Structure Constant Defines Visual Transparency of Graphene. *Science*.
- Nemes-Incze, P., Z. Osváth, K. Kamarás, and L. P. Biró (2008). Anomalies in thickness measurements of graphene and FLG crystals by tapping mode AFM. *Carbon*.
- Novoselov, K. S., A. K. Geim, S. V. Morozov, D. Jiang, Y. Zhang, S. V. Dubonos, I. V. Grigorieva, and A. A. Firsov (2004). Electric field effect in atomically thin carbon films. *Science* 306(5696), 666–669.
- Polat, E. O., O. Balci, N. Kakenov, H. B. Uzlu, C. Kocabas, and R. Dahiya (2015). Synthesis of large area graphene for high performance in flexible optoelectronic devices. *Scientific reports* 5, 16744.
- Regan, W., N. Alem, B. Aleman, B. Geng, C. Girit, L. Maserati, F. Wang, M. Crommie, and A. Zettl (2010, 3). A direct transfer of layer-area graphene. *Applied Physics Letters* 96(11).
- Reina, A., X. Jia, J. Ho, D. Nezich, H. Son, V. Bulovic, M. S. Dresselhaus, and J. Kong (2009). Large area, few-layer graphene films on arbitrary substrates by chemical vapor deposition. *Nano Letters* 9(1), 30–35. PMID: 19046078.
- Sakhaee-Pour, A. (2009, 01). Elastic properties of single-layered graphene sheet. *149*, 91–95.
- Seah, C. M., S. P. Chai, and A. R. Mohamed (2014). Mechanisms of graphene growth by chemical vapour deposition on transition metals.
- Smith, A. D., F. Niklaus, A. Paussa, S. Vaziri, A. C. Fischer, M. Sterner, F. Forsberg, A. Delin, D. Esseni, P. Palestri, M. Östling, and M. C. Lemme (2013). Electromechanical piezoresistive sensing in suspended graphene membranes. *Nano Letters* 13(7), 3237–3242.

- Smith, A. D., F. Niklaus, S. Vaziri, A. C. Fischer, M. Sterner, F. Forsberg, S. Schroder, M. Ostling, and M. C. Lemme (2014). Biaxial strain in suspended graphene membranes for piezoresistive sensing. *Proceedings of the IEEE International Conference on Micro Electro Mechanical Systems (MEMS)*, 1055–1058.
- Song, X., M. Oksanen, M. A. Sillanpää, H. G. Craighead, J. M. Parpia, and P. J. Hakonen (2012). Stamp transferred suspended graphene mechanical resonators for radio frequency electrical readout. *Nano Letters*.
- Sorkin, V. and Y. W. Zhang (2011). Graphene-based pressure nano-sensors. *Journal of Molecular Modeling*.
- Suk, J. W., A. Kitt, C. W. Magnuson, Y. Hao, S. Ahmed, J. An, A. K. Swan, B. B. Goldberg, and R. S. Ruoff (2011). Transfer of CVD-grown monolayer graphene onto arbitrary substrates. *ACS Nano* 5(9), 6916–6924.
- Tsioutsios, I., d. Bachtold, Adrian, and J. Pascual i Gainza (2016). *Mechanical resonators based on graphene and carbon nanotubes*. Ph. D. thesis, Universitat Autònoma de Barcelona, Barcelona.
- Van Der Zande, A. M., R. A. Barton, J. S. Alden, C. S. Ruiz-Vargas, W. S. Whitney, P. H. Pham, J. Park, J. M. Parpia, H. G. Craighead, and P. L. McEuen (2010). Large-scale arrays of single-layer graphene resonators. *Nano Letters*.
- Wei, X., B. Fragneaud, C. A. Marianetti, and J. W. Kysar (2009, Nov). Nonlinear elastic behavior of graphene: Ab initio calculations to continuum description. *Phys. Rev. B* 80, 205407.
- Yu, Q., J. Lian, S. Siriponglert, H. Li, Y. P. Chen, and S. S. Pei (2008). Graphene segregated on Ni surfaces and transferred to insulators. *Applied Physics Letters*.
- Yulaev, A., G. Cheng, A. R. Hight Walker, I. V. Vlassiouk, A. Myers, M. S. Leite, and A. Kolmakov (2016). Toward clean suspended CVD graphene. *RSC Advances*.
- Zhu, A. Y., F. Yi, J. C. Reed, H. Zhu, and E. Cubukcu (2014). Optoelectromechanical multimodal biosensor with graphene active region. *Nano Letters* 14(10), 5641–5649. PMID: 25184967.